Functional convergence of biosphere–atmosphere interactions in response to ~~meteorology~~meteorological conditions

Christopher Krich[1,2], Mirco Migliavacca[1], Diego G. Miralles[2], Guido Kraemer[1,3], Tarek S. El-Madany[1], Markus Reichstein[1], Jakob Runge[4], and Miguel D. Mahecha[3,5]

[1]Max Planck Institute for Biogeochemistry, 07745 Jena,Germany
[2]Hydro-Climate Extremes Lab (H-CEL), Faculty of Bioscience Engineering, Ghent University, Ghent, Belgium
[3]Remote Sensing Centre for Earth System Research, Leipzig University, 04103, Leipzig, Germany
[4]German Aerospace Center, Institute of Data Science, 07745, Jena, Germany
[5]Remote Sensing Centre for Earth System Research, Helmholtz Centre for Environmental Research UFZ, 04318 Leipzig, Germany

Correspondence: Christopher Krich (ckrich@bgc-jena.mpg.de)

Abstract. Understanding the dependencies of the terrestrial carbon and water cycle with meteorological conditions is a prerequisite to anticipate their behaviour under climate change conditions. However, terrestrial ecosystems and the atmosphere interact via a multitude of variables ~~, time- and space-~~ across temporal and spatial scales. Additionally ~~the~~ these interactions might differ among vegetation types or climatic regions. Today, novel algorithms aim to disentangle the causal structure behind such ~~interaction~~ interactions from empirical data. ~~Visualising the estimated structure in networks, the~~ The estimated causal structures can be interpreted as networks, where nodes represent relevant meteorological ~~determinants and~~ variables or land-surface fluxes, and the links the dependencies among them ~~possibly including their lag and strength~~(possibly including time-lags and link strength). Here we ~~show that~~ derived causal networks for different seasons at 119 eddy-covariance flux tower observations in the FLUXNET network. We show that the networks of biosphere–atmosphere interactions are strongly shaped by meteorological conditions. For example, we find that temperate and high latitude ecosystems during peak productivity exhibit very similar biosphere–atmosphere interaction networks as tropical forests. In times of anomalous conditions like ~~drought~~ droughts though, both ecosystems behave more like typical Mediterranean ecosystems during their dry season. Our results demonstrate that ecosystems from different climate zones or vegetation types have similar biosphere–atmosphere interactions if their meteorological conditions are similar. We anticipate our analysis to foster the use of network approaches as they allow a more comprehensive understanding of the state of ecosystem functioning. Long term or even irreversible changes in network structure are rare and thus can be indicators of fundamental functional ecosystem shifts.

1 Introduction

~~Ecosystems~~ Terrestrial ecosystems and the atmosphere constantly exchange energy, matter, and momentum (Bonan, 2015). These interactions result in biosphere–atmosphere fluxes (in particular carbon, water~~and sensible heat~~, and energy fluxes) that are shaped by a variety of climatic conditions and states of the terrestrial biosphere (McPherson, 2007). Understanding how biosphere–atmosphere fluxes interact and how they causally depend on the short-term meteorological and long-term climate

conditions is crucial for building predictive terrestrial biosphere models (Detto et al., 2012; Green et al., 2017). However, the exact causal structure of dependencies between surface and atmosphere variables is still subject to unknowns (Baldocchi et al., 2016; Miralles et al., 2019). For example, we still do not understand well under which conditions certain climate extremes turn ecosystems into carbon sources or sinks (Sippel et al., 2017; Flach et al., 2018; von Buttlar et al., 2018). One reason for our incomplete understanding is that the causal dependencies underlying biosphere–atmosphere interactions might vary among ecosystems ~~due to their structure and~~ depending on vegetation structure and its long-term adaptation to climatic conditions. ~~An other is that causal techniques are still rarely used. The~~

Conducting a comparative study across ecosystems, focusing on their interactions with the atmosphere has two requirements: Firstly, we need standardised data encoding biosphere fluxes and meteorological conditions. Secondly, an analytical tool is needed that extracts an interaction structure from these data empirically. The latter requires handling of multivariate processes and estimating dependencies beyond correlations. The first requirement is best met by the FLUXNET database (Baldocchi, 2014), a collection of global long-term observation of biosphere–atmosphere fluxes measured via the eddy covariance method ~~in FLUXNET (Baldocchi, 2014) should, however, allow us to disentangle such questions.~~

~~A variety of causal discovery methods have been developed over the past few years (see Runge et al., 2019a, for a recent overview). They allow to infer causal networks from empirical data enabled by certain general assumptions about the underlying processes. Some methods only consider two variables, such as (bivariate classical) Granger causality (Granger, 1969), convergent cross mapping (Sugihara et al., 2012), or transfer entropy (Schreiber, 2000). Other methods allow us to understand how multiple variables interact, accounting for common drivers and mediators by using conditioning approaches as suggested by multiple studies (Detto et al., 2012; Goodwell and Kumar, 2017; Papagiannopoulou et al., 2017a; Claessen et al., 2019; Runge et al., 2019b). One example for the latter is PCMCI , a~~ (Aubinet et al., 2012). The spatial distribution of FLUXNET sites is biased to European and North American sites, yet it still covers most climate zones and vegetation types ranging from boreal steppe to tropical rainforests surprisingly well Reichstein et al. (2014). Further, the data is processed homogeneously across sites. The second requirement is addressed by causal inference. Various methods exist today (see Runge et al., 2019a, for a recent overview), some of which have been applied already in the biogeosciences (Ruddell and Kumar, 2009; Detto et al., 2012; Green et al., 2017; Papagian One of that group is PCMCI (Runge et al., 2019b), a causal graph discovery algorithm based on a combination of the PC algorithm (named after its inventors Peter and Clark (Spirtes and Glymour, 1991)) and the Momentary Conditional Independence (MCI) test (Runge et al., 2019b). ~~Krich et al. (2020) showed that the PCMCI approach is useful to assess causal dependencies of ecosystem fluxes and atmospheric variables.~~ By applying such tests, it becomes possible to account for common drivers and mediators which can cause two variables to correlate even though, no direct causal link exists between them. Then MCI partial correlations estimated by PCMCI yield a better interpretation of the strength of a causal mechanism than the common Pearson correlation. Krich et al. (2020) tested PCMCI regarding its suitability for interpreting eddy covariance data. The method proved to be consistent despite the data's inherent noisy character and was capable to extract well interpretable interaction structures. A causal interpretation of specific links, though, has to take into account potentially unmet assumptions.

In this study, we ~~use~~ investigate multivariate time series from ~~global ecological observation networks such as FLUXNET to investigate how~~ FLUXNET tower data to understand how networks of biosphere–atmosphere interactions vary across veg-

etation types and climate zones. The rationale is as follows: If biosphere–atmosphere interactions ~~substantially vary~~ varied significantly across climate gradients or ~~among~~ between vegetation types, ~~then this may indicatethat~~ this could indicate, for example, that ecosystem responses to climatic extremes ~~may differ substantially and~~ could differ significantly and would require terrestrial biosphere models to account for them differently. If, however, the opposite applies and ecosystems of the Earth exhibit similar biosphere–atmosphere interaction types, then common principles can be identified that can serve as empirical reference for global vegetation models. ~~The assessment of these questions includes investigating the effect of extreme meteorological events on the network structure~~ We hypothesise first that the accessible states of biosphere–atmosphere interactions are limited and can be characterised by few functional states despite the complexity and differences among ecosystems.

~~To do so, we characterise biosphere–atmosphere interactions as weighted networks estimated via PCMCI (see Sect. 2.3). The nodes in these networks represent biosphere–atmosphere fluxes and meteorological variables (see Sect. 2.1). Any significant dependence among the variables is depicted as a link between the respective nodes and the link strength is measured by~~ Second, attributing to an ecosystems adaptation, we further hypothesise that specific ecosystem can only access a limited fraction of the ~~MCI partial correlation value (see Sect. 2.2). We estimated overall 10.038 networks from 119 ecosystemsusing sliding windows of three months over the available time-series length. This captures also an ecosystem's temporal development. Each of the estimated networks constitutes one high-dimensional observation with a network's links spanning the high dimensional space. Projecting this high dimensional space onto two dimensions using methods of non-linear dimensionality reduction (here t-SNE, see Sect. 2.4) reveals the dominant features of transitions between different statesof biosphere–atmosphere interactions, i. e. , which links are strong descriptors of differences between networks~~ functional states.

The study is designed as follows: Firstly, we perform causal discovery by PCMCI at each eddy covariance site and seasons. Secondly, we solely investigate the resulting interaction networks and visualise them in a low-dimensional space. We then ~~start with analysing the structure of the low dimensional embedding (Sect. 3.1). Subsequently we focus on ecosystem level behaviour, i.e. the seasonal median (Sect. 3.3) and individual years during extreme conditions (Sect. 3.4). Section 3.5 puts the results into broader perspective.~~ interpret the low-dimensional space of biosphere–atmosphere interactions and investigate seasonal cycles, characteristic states, the role of vegetation types and finally discuss the potential role of adaptation to the underlying climate space.

2 Data and Methods

2.1 Eddy-covariance observations

We used eddy covariance data from the FLUXNET database (Baldocchi et al., 2001) aggregated to daily time resolution. To maximise the available ecosystems and time series length, we took the union of the LaThuile Fair use (Baldocchi, 2008) and FLUXNET2015 Tier 1 (Pastorello et al., 2020) datasets (Nelson et al., 2020) with at least 5 years of measurement. If a site year was available in both datasets we selected the one from FLUXNET2015. A detailed list of used sites and years is given in table A1. The final dataset contains 119 sites from the major plant functional types and covers the major Koeppen-Geiger climate classes, i.e. tropical to polar climate zones. The majority of sites belong to evergreen needleleaf forests, grasslands

and deciduous broadleaf forests. The dominant climate classes are continental, temperate and dry climates. The dataset's variables, including meteorological and eddy covariance measurements, were quality checked, filtered, gap-filled, and partitioned with standard tools (Papale et al., 2006; Pastorello et al., 2020) and provided with per-variable quality flags. We extracted following variables, comparable between the two dataset, and their corresponding quality controls (if available): shortwave downward radiation (or global radiation, $R_{\overline{g}g}$), air temperature (T), net ecosystem exchange (NEE) (inverted, so that positive values signify carbon uptake into the biosphere), vapour pressure deficit (VPD), sensible heat- (H), latent heat flux (LE), gross primary productivity (GPP), precipitation (P) and soil water content (SWC, measured at the shallowest sensor). Within the FLUXNET2015 dataset these variables are named as: "SW_IN_F_MDS", "TA_F_MDS", "NEE_VUT_USTAR50", "VPD_F_MDS", "H_F_MDS", "LE_F_MDS", "GPP_NT_VUT_USTAR50", "P", "SWC_F_MDS_1", respectively. Correspondingly for the LaThuile dataset:"Rg_f", "Tair_f", "NEE_f", "VPD_f", "LE_f", "H_f", "GPP_f", "precip", "SWC1_f", respectively. GPP is calculated via the commonly used night time flux partitioning (Reichstein et al., 2005). Here GPP is the difference between ~~NEE and ecosystem respiration~~ ecosystem respiration and NEE. The latter is estimated via a model which is ~~parameterized~~ parameterised using night time values of NEE.

2.2 PCMCI

To analyse biosphere–atmosphere interactions, we estimated network structures using the causal network discovery algorithm PCMCI. PCMCI is tailored to estimate time-lagged dependencies from potentially high-dimensional and autocorrelated multivariate time series. Dependencies can be interpreted causally under certain assumptions. The algorithm is explained from a biogeoscience viewpoint in Krich et al. (2020). A comprehensive description from theoretical assumptions to numerical experiments is given in Runge et al. (2019b).

As a brief summary, PCMCI efficiently conducts conditional independence tests among ~~the contemporaneous (i.e. the dependence between two non-lagged variables) and time-lagged (up to some maximum time lag)~~ variables to reconstruct a dependency network. While PCMCI can also be combined with nonlinear tests, here we estimate conditional independence using partial correlation (ParCorr), implying that we only consider linear dependencies. Partial correlation between ~~X and Y given Z~~ two variables X and Y given a variable set Z is defined as the correlation between the residuals of ~~X and Y~~ X and Y after regressing out the (potentially multivariate) ~~condition Z~~conditions Z. The conditions Z can consist of lagged third variables or time-lags of X and Y.

PCMCI has two phases. In the first phase, the 'condition selection', a superset of lagged parents (up to some maximum time lag τ_{max}) of each variable, X_t^j, is estimated based on a fast variant of the PC algorithm (Spirtes and Glymour, 1991). A parent of X_t^j is any lagged variable, $X_{t-\tau}^i$, that is directly influencing X_t^j. This can be the own past, $i = j, \tau > 0$ or other variables, $i \neq j, \tau > 0$. A pseudo-code of this procedure is given in the supplementary materials of Runge et al. (2019b). In the second phase, 'momentary conditional independence' (MCI) is estimated among all pairs of contemporaneous and lagged variables $(X_{t-\tau}^i, X_t^j)$ for $\tau \geq 0$~~is estimated~~. The MCI test removes the influence of the lagged drivers (obtained in the first phase) ~~and yields~~ using ParCorr and yields link strengths and p-values (based on a two-sided t-test)~~for causal links among each time-lagged and contemporaneous variable pair. The strength of links~~ . The link strength is here given by the MCI partial

correlation . In short, the MCI value gives an estimate of dependence between two time series, one potentially lagged, with the influence of other lagged drivers including autocorrelation removed, yielding a better interpretation of the strength of a causal mechanism than the common Pearson correlation. For a more detailed discussion of the interpretation, see Runge et al. (2019b). As a particular partial correlation, the MCI value is independent of the variables' mean value and is normalised in [-1, 1] and can, hence, be compared between variable pairs with different units of measurement. Lagged links are directed forward in time~~and contemporaneous~~ . Contemporaneous dependencies are left undirected as no time information reveals the direction of influence unless they are defined as unidirectional by the user (pcmci parameter selected_links, see table B1). A causal interpretation of links rests on the standard assumptions of causal discovery. Here we assume time order, the causal Markov condition, faithfulness, causal sufficiency, causal stationarity, and no contemporaneous causal effects. The use of ParCorr additionally requires stationarity in the mean and variance and linear dependencies (Runge et al., 2019b). In particular, a statistical independence (here at a 0.1 two-sided significance level) between a pair of variables conditional on the other lagged variables is interpreted as the absence of a causal link (Faithfulness condition). On the other hand, a causal interpretation of the estimated links is here to be understood only with respect to the variables included in the analysis. ~~Unobserved common drivers can still render links as spurious. In the present context we aim to classify networks and a causal interpretation of each link is not the focus.~~ The dependence structure among variables can finally be visualised by weighted networks with ~~link weights given by the MCI partial correlation. MCI partial correlation removes the influence of other lagged drivers and autocorrelation, yielding a better interpretation of the strength of a causal mechanism than the common Pearson correlation. At the same time,~~ the nodes representing the variables and the links significant dependencies with its strengths given by the MCI partial correlation~~values are normalised in -1, 1and can, hence, well be compared between variable pairs with different units of measurement~~.

2.3 Network Estimation

~~Networks~~

Dependencies are estimated using PCMCI ~~between~~ among the variables $R_{\overline{g}g}$, T, NEE, VPD, H and LE using time lags ~~between~~ ranging from zero to five~~days (see Supplementary Material Table B1 for settings)~~. As was already discussed by Krich et al. (2020), eddy covariance data and the choice of our variable set do not fully fulfil all assumptions of PCMCI. Causal sufficiency and no contemporaneous links are obviously not fulfilled which can lead to spurious links. Yet, in the present context we aim to compare networks and a causal interpretation of each link is not the focus. We further can not rule out non-linear dependencies. In case they have a strong linear part, we nevertheless can detect them. Based on findings in Krich et al. (2020), we subtracted a smoothed seasonal mean from each variable to remove the common driver influence of the seasonal cycle that would yield spurious dependencies. The seasonal mean was smoothed by setting the high frequency components (> 20 days^{-}) of its Fourier transform to zero. This decreases the detection of false links while leaving the detection of true links largely unaffected. We estimated networks in sliding windows of three months, taking the centre month as the time index of each network. The sliding windows help to capture the temporal evolution of biosphere–atmosphere interactions and provide enough data points for the network estimation via PCMCI. Additionally, we improve stationarity of the data further

and address the requirement of causal stationarity, i.e. a causal link persists throughout the time period of network estimation. Further we set R_g as a potential driver of the system (by excluding its parents from the PCMCI parameter 'selected_links', see table B1). We acknowledge the possibility of R_g being influenced by other variables, e.g. via transpiration and subsequent cloud formation. Yet, on the ecosystem scale we work with, we presume this effect to be rather small and likely dominated by lateral transport. Besides these possibilities, setting R_g as driver can account for remaining non stationarities (Runge, 2018). Missing data was flagged as such and is ignored by PCMCI. To avoid effects on the network structure from gap-filling we used the following quality flag thresholds. A daily datapoint is not used if its quality flag is below 0.6 (i.e. more than 60% of measured and good quality gap filled data). In case more than 25% of datapoints of the three month window are flagged as bad quality, the time window is removed from the analysis. To analyse the factors influencing network structure, we consider the mean values over the respective time period of the variables included in the network calculation, and additionally those of GPP, P and SWC. GPP, P and SWC were not included in the network calculation because certain characteristics can impinge on network estimation. GPP is derived using NEE and T. Any of the links GPP–T and GPP–NEE thus could be due to its processing rather than an actual dependence. P, on the other hand, typically yields non intuitive results due to its binary character (precipitation of a certain amount - ~~no precipitation).~~ zero precipitation), while its effects occur more smoothly (e.g. increase in transpiration or respiration) and its strong deviation from a normal distribution. Further, it can happen that over the time period of network estimation no precipitation occurs rendering such periods not analysable. The issue with SWC is its lower availability and for those sites that have such measurements it might be applied at differing depth. The depth that is mostly present is at shallow depths of 5 or 10 cm. The upper soil layer, however, dries out quickly and can explain only little of the latent heat flux.

2.4 Dimensionality Reduction

~~Applying above described procedure we obtained 10.038 networks for the different months and sites. Each network, with 6 variables and 6 time lags, contains 216 links and can, hence, be embedded into a 216 dimensional space. However, here we only focus on the 15 contemporaneous links since we found them to be strongest and most robust. Therefore, the dimensionality reduction step was performed on those links only .~~ For the dimensionality reduction, we tested principal component analysis (PCA; Pearson, 1901), t-distributed stochastic neighbour embedding (t-SNE; Maaten and Hinton, 2008), and uniform manifold approximation and projection (UMAP; McInnes et al., 2018). PCA is the standard method for dimensionality reduction, it is commonly used, linear, fast, and easily interpretable regarding the meaning of its axes (the principal components). A PCA embedding typically fails to reveal complex clusterings, because it maintains large scale gradients but often produces embeddings in which far away points appear very close in the embedding. In contrast t-SNE ~~preserves local neighbourhoodswhich makes it~~ aims to preserve local neighbourhoods. Therefore it calculates first similarity scores for each point pair using euclidean distances and Gaussian distributions. Subsequently it randomly projects the data onto the lower dimensional space and attempts to rearrange points in a way that the previously determined similarities are obtained. To assess the similarities in the low dimensional space, however, it uses a Student-t distribution. This helps to separate points which are also originally separated. This procedure makes t-SNE very good at visualising clusters in the data and non-linear relationships. Drawbacks are the difficult interpretability of the embedding axes due to the non-linear nature and its fairly long computation time for large

datasets. Further, distances between far separated points and those belonging to different clusters in the embedding space are not (necessarily) comparable to the original distances. This is as t-SNE does not preserve both the global and local structure at the same time, which is attempted by UMAP. UMAP was developed as an improvement of t-SNE regarding ~~computation time while having an embedding with similar properties as~~ structure preservation and results also in a shorter run time especially for higher dimensions. A comparison of t-SNE and UMAP is given in appendix C in McInnes et al. (2018). According to Kobak and Linderman (2019), the global structure preservation of UMAP is not an inherent characteristic of the method itself but rather stems from the choosen initialization.

As we are dealing with an unsupervised method there is no obvious measure to assess the quality of an embedding, as each method optimises a different error function. A measure commonly used for the comparison and characterisation of dimensionality methods is the agreement between K-ary neighborhoods (the K nearest points to an observation) in the high dimensional and low dimensional space. The measure $R_{\mathrm{NX}}(K)$ (Lee et al., 2015) gives a measure of the improvement of the embedding of K-ary neighborhoods over random embeddings. For an embedding with random coordinates we obtain $R_{\mathrm{NX}}(K) \approx 0$ and if the K-ary neighborhoods are perfectly preserved we obtain $R_{\mathrm{NX}}(K) = 1$. As this measure depends on the neighborhood size, K, we can draw a curve over K that characterizes if the method is better at maintaining global or local neighborhoods. The area under the $R_{\mathrm{NX}}(K)$ curve gives an idea of the overall quality of the embedding. An intercomparison of the three dimensionality reduction methods using this measure shows t-SNE to perform best (see Fig. A1, B1, C1).

2.5 Distance Correlation

Distance correlation (Székely et al., 2007) is a non linear measure to quantify the dependence between two vectors. It has been used successfully to assess the influence of variables on the low dimensional embedding (Kraemer et al., 2020b). Székely et al. (2007) detail its empirical definition for a sample $(\mathbf{X}, \mathbf{Y}) = \{(X_k, Y_k) : k = 1, ..., n\}$ with $\mathbf{X} \in \mathbb{R}^p$ and $\mathbf{Y} \in \mathbb{R}^q$ as follows:

$$\mathcal{R}_n^2(\mathbf{X}, \mathbf{Y}) = \begin{cases} \sqrt{\frac{\mathcal{V}_n^2(\mathbf{X},\mathbf{Y})}{\mathcal{V}_n^2(\mathbf{X},\mathbf{X})\mathcal{V}_n^2(\mathbf{Y},\mathbf{Y})}}, & \mathcal{V}_n^2(\mathbf{X},\mathbf{X})\mathcal{V}_n^2(\mathbf{Y},\mathbf{Y}) > 0, \\ 0, & \mathcal{V}_n^2(\mathbf{X},\mathbf{X})\mathcal{V}_n^2(\mathbf{Y},\mathbf{Y}) = 0. \end{cases}$$

where $\mathcal{V}_n^2(\mathbf{X}, \mathbf{Y})$ is the empirical distance covariance with $\mathcal{V}_n^2(\mathbf{X}, \mathbf{Y}) = \frac{1}{n^2}\sum_{k,l=1}^{n} A_{kl}B_{kl}$. A_{kl} and B_{kl} are distance matrices defined by

$$A_{kl} = a_{kl} - \bar{a}_k - \bar{a}_l + \bar{a}, \qquad \bar{a} = \frac{1}{n^2}\sum_{k,l=1}^{n} a_{kl}, \qquad \bar{a}_k = \frac{1}{n}\sum_{k=1}^{n} a_{kl}, \qquad \bar{a}_l = \frac{1}{n}\sum_{l=1}^{n} a_{kl}, \qquad a_{kl} = |X_k - X_l|_p$$

Distance correlation can be used to quantify the dependence between two sets of observations of differing dimensionality. In our case these two vectors are firstly a link strength or a underlying quantity of the networks (1d) and secondly the networks' position in the low dimensional embedding (2d). The resulting dependence value is used to rank the quantities in their ability to describe the structure of the low dimensional embedding.

2.6 Clustering and median network trajectories

On the reduced space we applied a clustering method named Ordering Points To Identify the Clustering Structure (OPTICS; Ankerst et al., 1999). ~~Clusters are found~~ OPTICS finds clusters by identifying regions of high density that contain a certain number of datapoints ($min_{samples}$). The cluster borders are defined by a certain drop in reachability of further datapoints (max_{eps} and xi). This allows points that lie outside the reachability of neighbouring clusters to remain unclustered. ~~Following~~ The following settings were used for clustering: $min_{~~samples~~}$ samples=80, $max_{~~eps~~}$ eps=8 and xi=0.5. We calculated mean networks for each cluster by calculating the mean MCI value for each contemporaneous link ~~of each network~~ among all networks contained in the cluster and only took those links that had an absolute value above 0.2.

2.7 Visualising ecosystem trajectories

As we calculated networks for each month for each measurement year for each FLUXNET site (if data requirements are fulfilled, see Sect. 2.3), annual trajectories can be visualised in the low dimensional embedding by connecting the dots representing the monthly networks of a specific year. Further, for each ecosystem, we calculated ~~an annual~~ a monthly median trajectory within the t-SNE space which is composed of its monthly median networks. To this end, we calculated ~~non-intercepting~~ non-intersecting convex hulls which consisted of at least three datapoints (networks within the t-SNE space belonging to the same ecosystem, representing the same month, in at least three years). The monthly median network is the average of the networks lying on (≥ 3 networks) or in the inner hull (< 3 networks).

2.8 Workflow

Our restrictions on the data length and quality resulted in a selection of 119 FLUXNET sites (Fig. 1a). Applying above described procedure we obtained 10.038 networks for the different months and sites. An example network estimated by PCMCI is shown in Fig. 1c. The strongest and most consistent links are contemporaneous, indicating that interactions happen on time scales shorter than the time resolution. While lagged common drivers are excluded, contemporaneous links can still be spurious due to contemporaneous confounding (see Sect. 2.2). Nevertheless, we focus our analysis on these 15 links, as they contain most information. This is done by performing the dimensionality reduction on contemporaneous links and neglecting the lagged ones. The rational of employing a dimensionality reduction is the following. Each of the estimated networks constitutes one observation in a high dimensional space with a network's links spanning its axes (Fig. 1d). Projecting this high dimensional space onto two dimensions (Fig. 1e) allows first of all for visualisation. In case the data consists of a structure that can be 'identified' by the dimensionality reduction method, the visualisation reveals the dominant features of transitions between different states of biosphere–atmosphere interactions. The dominant features are the links that appear with strong gradients in the low dimensional embedding. To quantify and later rank the gradients exhibited by each link, we use the measure distance correlation (see Sect. 2.5). Therefore, we calculate the distance correlation of the link strengths (1d) with their position on the low dimensional embedding axes (2d). We also examine the distance correlation of secondary quantities with the axes. The secondary quantities are firstly mean values of variables calculated for each three month period of network estimation as well

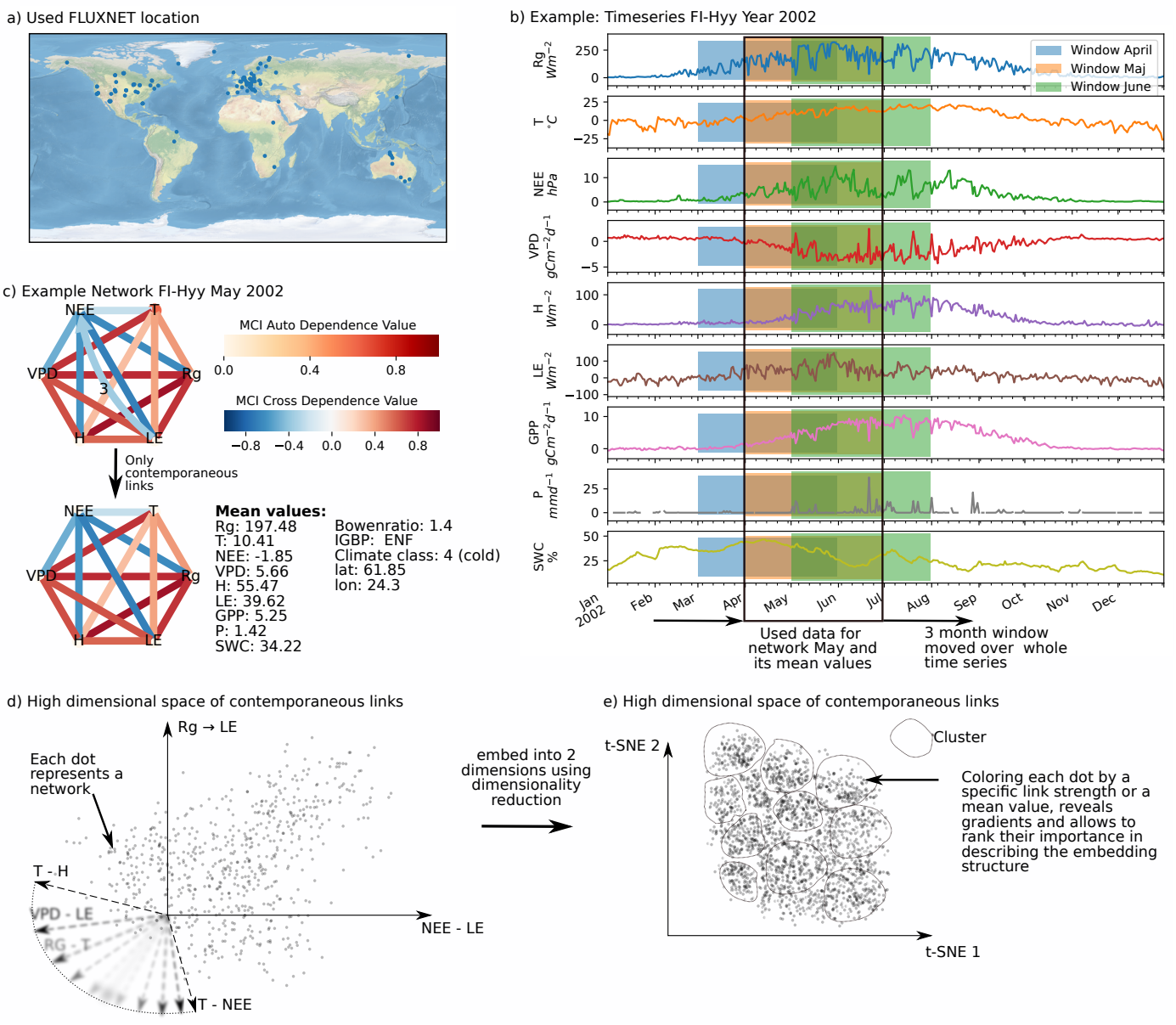

Figure 1. Schematic representation of the workflow. a) Eddy covariance data from the FLUXNET database are selected (119 sites). b) For each site we used the time series of global radiation R_g, air temperature T, vapour pressure deficit VPD, net ecosystem exchange NEE, sensible heat H, latent heat LE, gross primary productivity GPP, precipitation P and sail water content SWC. Networks are estimated in three month moving windows using Rg, T, NEE, VPD, LE and H. c) An example interaction network for FI-Hyy May 2002. The strongest and most persistent links are contemporaneous (i.e. undirected). Thus we limit our analysis to those links. d) Each three-month network can be interpreted as an observation in a 15-dimensional space (each contemporaneous link is one dimension). e) Dimensionality reduction projects all interaction networks into a two dimensional space preserving its local neighbourhood structure. Here any subsequent analysis and interpretation will be realised.

as secondly static values like climate class, vegetation type or location. The secondary quantities are used to find covariates of the low dimensional embedding that can help to explain its structure. In a next step, we cluster the low dimensional embedding to further understand to which network structures the gradients of link strength lead (see Sect. 2.4) and calculate the cluster's average networks (a simple mean). Up to this point (Sect. 3.1 and 3.2), we analysed the manifold of biosphere–atmosphere interactions and can address the first part of our hypothesis. As each point of the low dimensional embedding represents the biosphere–atmosphere interactions of a specific ecosystem at a specific time we can investigate the behaviour of specific ecosystems (see Sect. 2.7). Therefore we look at the monthly median and annual trajectories of certain ecosystems (Sect. 3.3 and 3.4). This leads to the answer of the second part of our hypothesis.

3 Results and Discussions

3.1 Two-dimensional embedding of biosphere–atmosphere networks

~~The~~ To find the most suitable dimensionality reduction method, we evaluated three different methods (PCA, t-SNE ~~performed best at projecting~~ and UMAP) with respect to their ability to project the high dimensional ~~space created by the networks contemporaneous links~~ network space onto two dimensions. To compare the low-dimensional embedding spaces, we used the $R_{\mathrm{NX}}(K)$ measure (see Sect. 2.4) which quantifies how well neighbourhoods are preserved when projecting the high dimensional space onto fewer dimensions. We found that t-SNE achieved the best projection, by best preserving both local and distant neighbourhoods (cf. Sect. 2.4, Fig. A1, B1). This is unexpected as UMAP is said to intentionally preserve the global structure. Yet, as can be seen in Fig. 4a, the networks almost form a continuum. Thus, by maintaining the local neighbourhood structure, also the global structure is preserved within t-SNE.

The two-dimensional embedding by t-SNE of biosphere–atmosphere interactions is ordered primarily by dependencies including carbon flux (NEE) and energy distributions (LE, H). This can be seen in Fig. 2 which shows the ~~embedding colour coded~~ 2d embedding colour-coded by the strength of individual links, i.e. MCI partial correlation values. The colouring reveals that the link strengths are ordered along gradients~~. The strongest gradients measured via distance correlations (Székely et al., 2007) are given by~~ , i.e. they exhibit some dependence with the t-SNE axes. Using distance correlation to rank those gradients (see Sect. 2.5), we find the links NEE–LE ($\rho = 0.75$~~$\mathcal{R} = 0.75$~~), Rg–LE ($\rho = 0.73$~~$\mathcal{R} = 0.73$~~) and T–H ($\rho = 0.69$~~$\mathcal{R} = 0.69$~~) to have the strongest gradients. The connection between carbon and water fluxes as well as the role of energy input to sustain water fluxes (if available in the soil) are well known and investigated dependencies (Beer et al., 2010; Luyssaert et al., 2007). ~~Further, gradients of mean climatic conditions emerge. This is depicted in Fig. 3 showing again the low dimensional embedding, this time colour coded~~

To search for covariates that help to explain - and if thought further, help to predict the network structures- we colour coded the embedding by the networks' underlying mean conditions, i.e. the average over the respective time window, of the exchange rates (GPP, NEE, LE and H) as well as meteorological conditions (Rg, T, VPD, P). This is shown in Fig. 3. Clearly, the mean exchange rates and meteorological conditions - although not considered in the estimation of the networks - are related to the observed biosphere–atmosphere interactions. On the contrary, corresponding vegetation types and Köppen-Geiger classes are

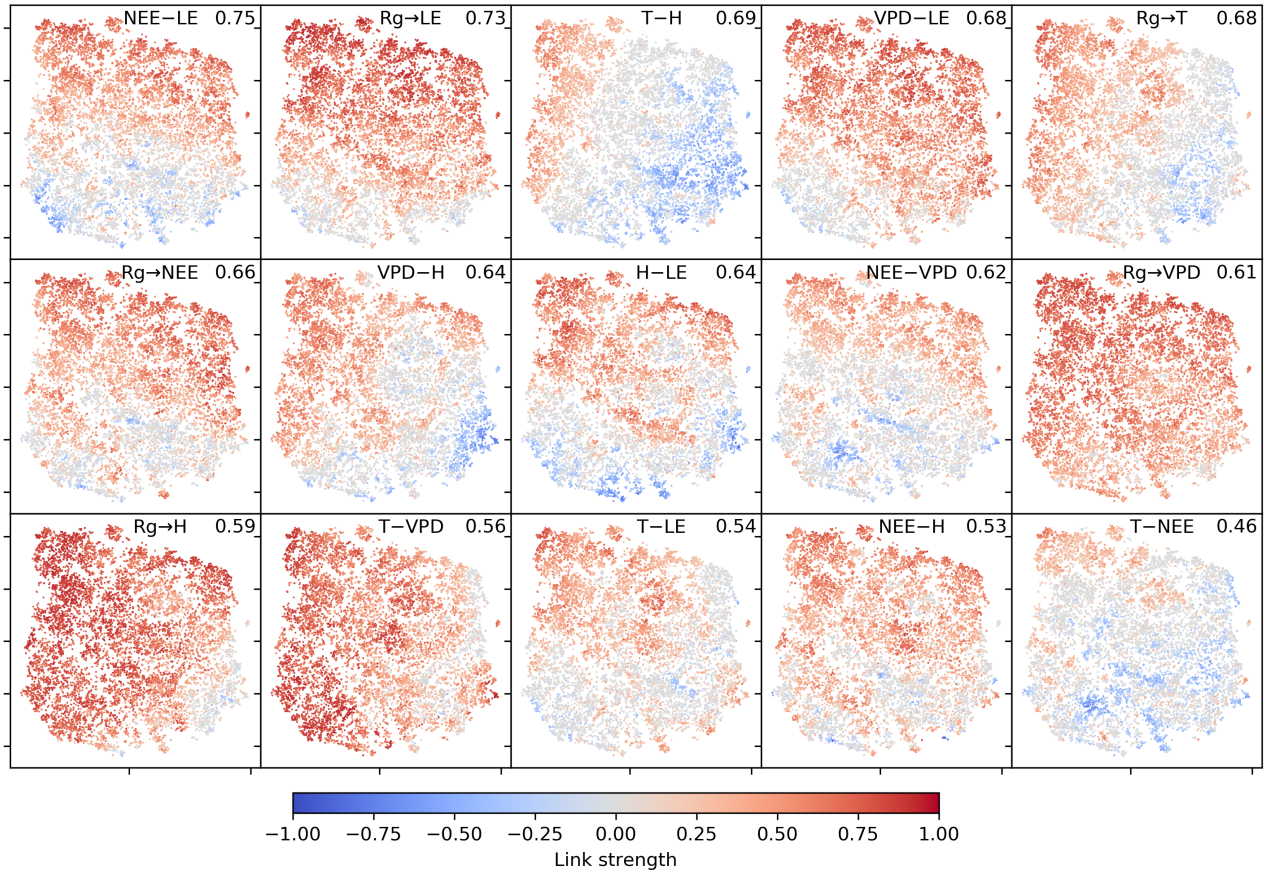

Figure 2. Two-dimensional embedding of three-monthly biosphere–atmosphere networks realised via t-SNE. Shown is the distribution of link strengths among the networks. The strength is estimated via MCI partial correlation values. Subfigures are sorted by the distance correlation of the link's MCI value with the axes (value in upper right corner). As R_g ~~can only be a cause~~is set as potential driver (PCMCI parameter 'selected_links', see table B1), connections including R_g are directed $\rightarrow$.

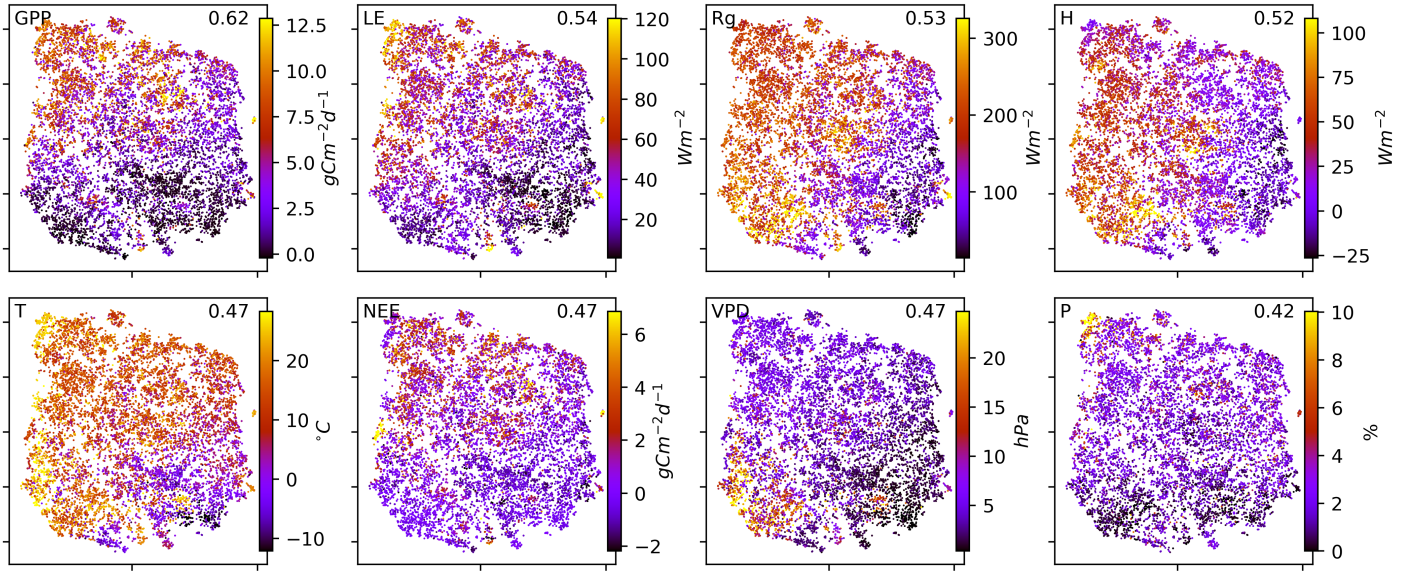

Figure 3. Two-dimensional embedding coloured by underlying mean exchange rates and meteorological conditions. The mean values are calculated over the respective time periods used for the network estimation. Each network is estimated on a three month window of daily time series data. Values are cut off at the highest and lowest percentile.

not as much related as displayed in the Supplementary Material section Fig. D2. The results show that a high dimensional space encompassing more than 10000 ecosystem networks representing the states of biosphere–atmosphere interactions from ecosystems of various geographic origins can be reduced to a compact two dimensional manifold characterised by four edges and gradients of mean biosphere and atmosphere conditions. While gradients in MCI partial correlation strength are expected as they were used as features in the dimensionality reduction, gradients in mean climatic and biospheric conditions were not. This information thus must be entailed in the networks' structure. To better grasp the distribution of network structures, we further analyse the emerging clusters.

3.2 Clusters of characteristic ecosystem–atmosphere networks

As we apply a significance threshold to each link of the estimated network structures (see Sect. 2.3), the networks typically lack weak links. This leads to a certain degree of clustering among the networks, which we identified using the OPTICS approach (see Sect. 2.6; Ankerst et al., 1999)) (Fig. 4a). Cluster boundaries are shown by the convex hulls in Fig. 4b, where we also visualise the mean ~~interaction~~ networks of each cluster. ~~Based on this analysis we can identify four~~ This visualisation reveals

that the mean networks of the clusters situated at the embedding's edges can be regarded as archetypes of network structures, i.e. extremal, characteristic states (similar to the concept of endmember states). The four states can be described as follows:

Type 1 is a sparsely connected network. Links, if present, are very weak and predominantly exist among atmospheric variables. Mean atmospheric conditions are characterised by low energy input (low R_g and T). Carbon and water fluxes are consequently close to zero, and daily averages of sensible heat can even reach negative values. Such conditions reflect high latitude ecosystem winter states experienced by ecosystems like the evergreen needle ~~leave~~ leaf forests (ENF) of Finnland, i.e. Hyytiälä (FI-Hyy) and Sodankyla (FI-Sod) as well as Canada, i.e., the UCI-1850 burn site (CA-NS1) and Quebec - Eastern Boreal (CA-Qcu) during December and January.

Type 2 consists of strong links among atmospheric variables but LE and NEE are weakly, not, or even negatively connected to the atmosphere, i.e. the meteorological variables. This network structure coincides with high energy input (high R_g and T) but low water availability (low P and SWC, high VPD). A high Bowen ratio, i.e. the ratio between sensible heat and latent heat, representing aridity, and low ~~carbon fluxes~~ absolute carbon fluxes (GPP and NEE) are the consequence. These conditions are typically present at semi-arid ecosystems like the woody savanna (WSA) Santa Rita Mesquite (US-SRM) as well as the grasslands Santa Rita (US-SRG), Audubon Research Ranch (US-Aud) and Sturt Plains (AU-Stp) during dry season.

Type 3 exhibits the same strong links among Rg, VPD and H as Type 2 but T is weakly or not connected~~and the opposite for~~. The opposite is true for links of LE and NEE which are strongly connected to the other variables (except T). R_g and T are considerably lower than in Type 2 (approximately by 100 W/m^2 and 10°C) but because of sufficient water availability the Bowen ratio is between 0 and 1. Typical ecosystems in this state are mid to high latitude forests during spring or autumn, e.g. Harvard Forest EMS Tower (US-Ha1, deciduous broadleaf forest (DBF)), Roccarespampani 1 (IT-Ro1, DBF), Vielsalm (BE-Vie, mixed forest (MF)) and Hyytiälä (FI-Hyy, ENF).

Type 4 is fully and strongly connected. Both energy input and water availability are high leading to Bowen ratios around 1. This network state is typically present in tropical forests like the Guyaflux site in French Guiana (GF-Guy) (evergreen broadleaf forest (EBF)) but can temporarily be also reached by a variety of other ecosystems, e.g. mid and high latitude forests like Hainich (DE-Hai, DBF), Tharandt (DE-Tha, ENF), BE-Vie (MF), FI-Hyy (ENF) as well as woody savannas (WSA) as Howard Springs (AU-How) and grasslands as Daly River Savanna (AU-Dap).

The archetypes of networks are located at the edges of the two-dimensional space and thus could define two imaginary axes. From a physical point of view, energy is required for each process and interaction to occur, e.g. photosynthesis or evaporation (Bonan, 2015). Therefore, transitions along the axis connecting the network types 1 and 4 might be interpreted as energy controlled as dependencies among all variables fade or increase consistently. Transitions along the axis connecting network types 2 and 3 are explainable by a combination of water availability and a temperature gradient. Low water availability but high temperatures ~~lead~~ cause shut down of stomatal conductance or ecosystems to enter a dormant state which leads to low carbon and water fluxes and ~~thus~~ low connectivity. On the other hand, sufficient water and medium temperatures ~~allow for~~

fluxes but likely (around the optimum of photosynthesis) allow for carbon and water fluxes but reduce the influence of varying temperatures leading to connected NEE and LE but disconnected T. And indeed these patterns and gradients exist. Mean R_g is lowest at network type 1 and almost linearly increases towards network type 4. P is lowest at network type 1 and 2. In combination with high energy input network type 2 has lowest SWC values and the highest Bowen ratios (see Supplementary Material section Fig. D2). SWC is higher but quite dispersed elsewhere suggesting that at a certain point water limitations are fading out. T values of course also show an increase from network type 1 to 4 (as radiation) but also from network type 3 to 2 and are actually rather low (8°C to 15 °C) at network type 3 (see Fig 3). As meteorological conditions affect biosphere productivity, network type 1 and 2 exhibit low, type 3 medium and type 4 high productivity i.e. estimated as GPP. In short, the clustering revealed that changes in energy and water availability can explain major transitions between different states of biosphere–atmosphere interactions. This is in line with a recent study showing that a variety of land-surface processes can be largely summarised by on the one hand productivity measures and on the other hand water and energy availability. Both, water and energy availability, need to be high for high productive states, yet the lack of either of them leads to low productivity (Kraemer et al., 2020a). This biosphere state triangle is found in our analysis by the network type 1 (cold - low connectivity), 2 (dry - NEE/LE weakly connected) and 4 (high productivity - fully connected). Yet, a fourth network type (type 3) is naturally occurring in the t-SNE space as we here include interactions with the atmosphere.

Up to this point we have found strong evidence supporting our first hypothesis. The manifold of biosphere–atmosphere interactions can be represented rather well by two dimensions which we identified to be most consistent with energy and water availabilities. It is confined by four characteristic states and populated homogeneously by the observed network states. Having an understanding of the low dimensional embedding's structure now allows us to analyse specific ecosystem behaviour.

3.3 Ecosystems' median trajectories

Each point in the reduced t-SNE space represents a biosphere–atmosphere interaction network for a given month and ecosystem. Hence, we can trace an ecosystem's trajectory through time. An We are first focusing on an ecosystem's median annual monthly trajectory (see Sect. 2.62.7) within the low dimensional spacereflects . We can see that the median trajectories reflect seasonal patterns of meteorological conditions (Fig. 5). For example, mid-latitude sites like FR-Pue (EBF), DE-Hai (DBF) and FI-Hyy (ENF) exhibit a strong seasonal variation of $R_{\overline{g}\,g}$ and span a long distance in the t-SNE space. In contrast, tropical ecosystems like GF-Guy (EBF) constantly have high $R_{\overline{g}\,g}$ and exhibit predominantly network type 4 indicative of high productive conditions - while DE-Hai or FI-Hyy reach this connectivity pattern only during peak growing season. US-SRM (WSA), however, has similar or even higher $R_{\overline{g}\,g}$ values throughout the year but barely manages to deviate from type 2 which is in accordance with its low water availability. The amount of precipitation further aligns with differences and characteristics of the trajectories of FR-Pue, DE-Hai and FI-Hyy. For example, FI-Hyy shows some deviation towards edge 2 in February and March, FR-Pue in June, July and August. For both, mean precipitation is lowest during these month. The strong control by energy and water availability is in line with a recent analysis showing that variability in land-surface processes is largely explained by productivity measures as well as water and energy availability. Both, water and energy availability, need to be high for high productive states, yet the lack of either of them leads to low productivity (Kraemer et al., 2020a). This biosphere

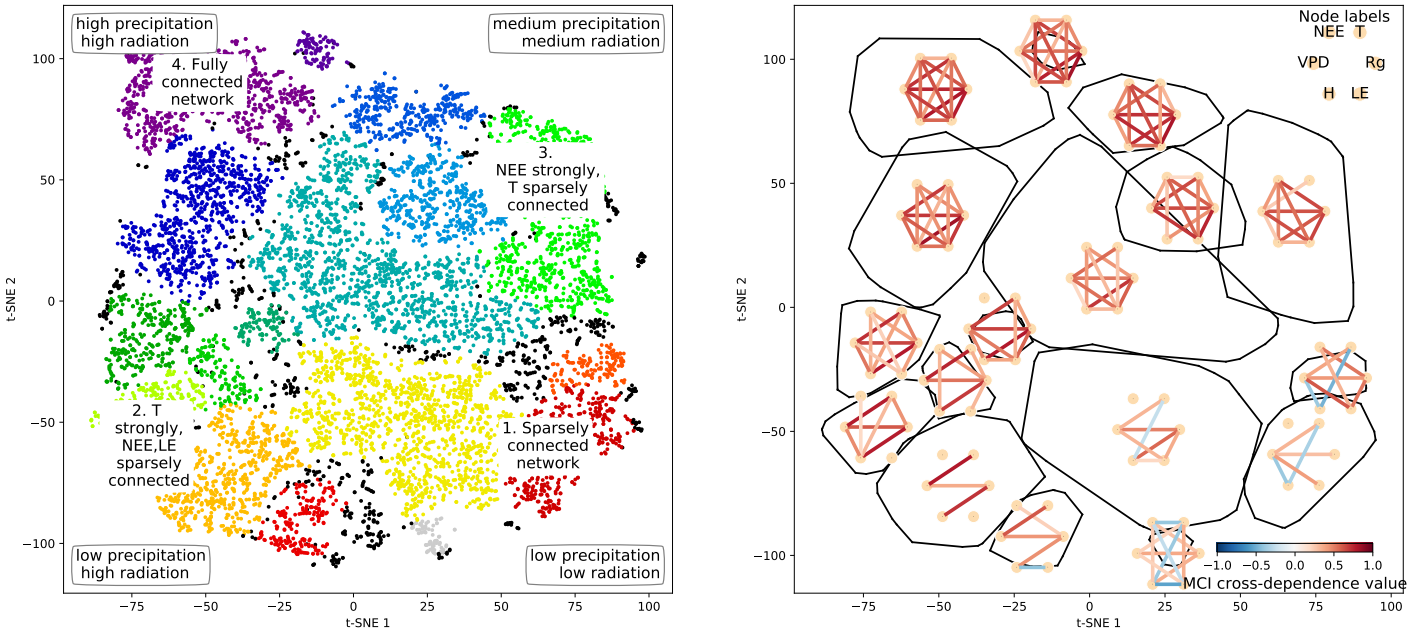

Figure 4. Structure of the two-dimensional embedding. left: t-SNE space clustered by the OPTICS approach (Ankerst et al., 1999). Colours represent different clusters, black dots are not attributed to a cluster. Indicated are the four archetypes of network connectivity and the networks underlying meteorological conditions. right: Convex hulls of clusters and their average network, i.e. average over all networks belonging to one cluster. Average networks are thresholded at a minimum link strength of 0.2. A finer clustering can be found in the Supplementary Material section Fig. D1.

~~state triangle is found in our analysis by the network type 1 (cold), 2 (dry) and 4 (high productivity). Yet, a fourth network type (type 3) is naturally occurring in the t-SNE space as we here include interactions with the atmosphere~~months. These behaviours demonstrate what the previous figures (Fig. 3 and 4) have already suggested: Ecosystem's populate the low dimensional space and migrate within as allowed by their climatic conditions. Thereby they can exhibit a wide range of interaction structures as can be seen from the mid-latitude sites. As these behaviours are multi year averages they could resemble more ecosystem adaptation to median climatic conditions than flexible adjustment of biosphere–atmosphere interactions to quickly changing meteorological conditions. If biosphere–atmosphere interactions are confined by adaptation shall be investigated in the final analysis section.

3.4 Deviations from ecosystem median trajectories

~~Climatic extremes are visible in an ecosystem's trajectory as strong deviations from the median trajectory~~The remaining open question is, how flexible do the networks adjust to deviations from mean climatic conditions. Therefore, we look at climatic anomalies. Figure 6 shows the trajectories of ecosystems during anomalous dry or wet conditions. During the European heat-wave of 2003, in July and August the trajectories of two temperate central European forests, DE-Hai and DE-Tha, no longer

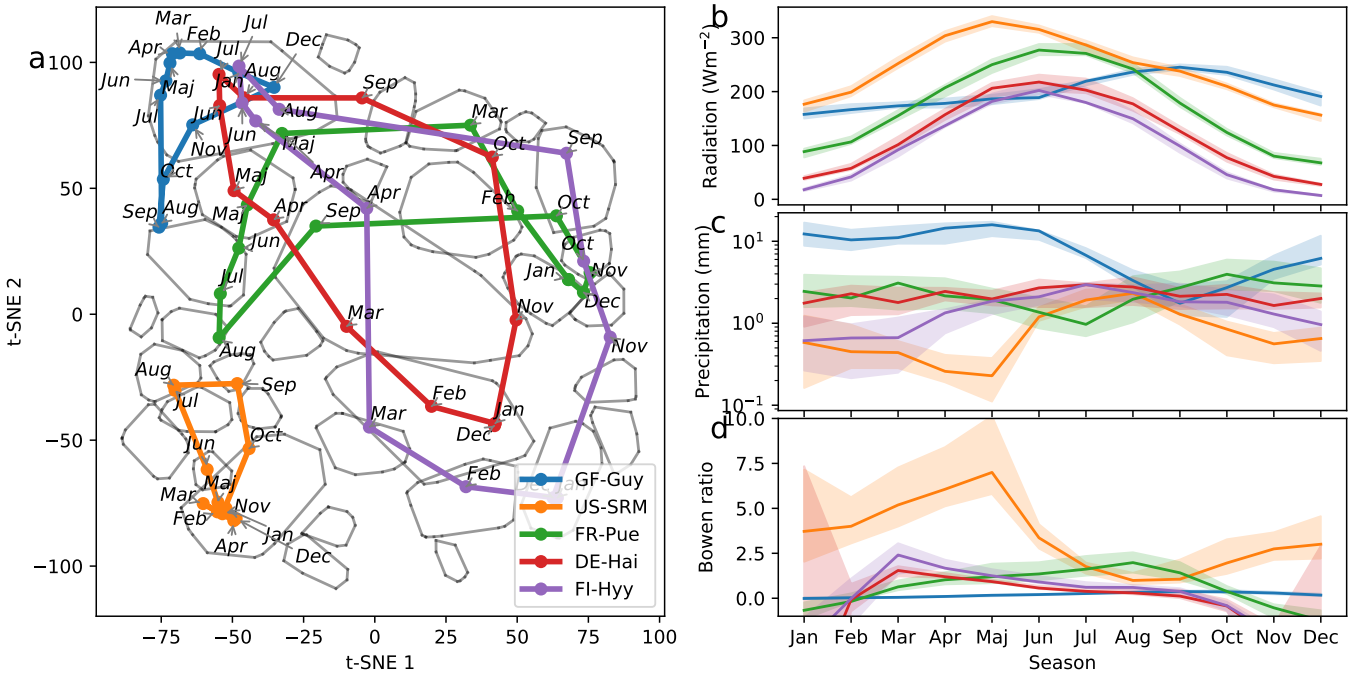

Figure 5. Median trajectories of selected sites (left) and their corresponding mean values of radiation, precipitation and the Bowen ratio (right). In winter month the Bowen ratio can turn negative. Nevertheless we set the lower limit of the y-axis to 0. As networks are calculated using a centred three month moving window, each month is ascribed a network. Thus, the behaviour of an ecosystem can be tracked by its monthly networks, which form trajectories for each year. An ecosystem's monthly median trajectory is composed of the two dimensional monthly median networks (see Sect. ~~2.6~~ 2.7 for details).

manage to establish a network structure resembling network type 4, typical for these ecosystems during their high productive phase. Instead they are shifted towards network type 2, associated with drier conditions (Fig. 6a, b). Similarly, the ecosystem BR-Sa3 (EBF) in the Brazilian tropical rainforest shows substantial deviations towards network type 2 during the exceptional dry season of 2001 (Aug, Sep, Oct) (Marengo et al., 2018) (Fig. 6c). In contrast, US-Wkg is a grassland accustomed to dry conditions and thus predominantly exhibits low water and carbon fluxes resulting in network structures as of network type 2, i.e. water and carbon fluxes are barely or even disconnected. Carbon and water fluxes of semi-arid ecosystems, however, are known to respond quickly and strongly to sufficient precipitation (Potts et al., 2019; Leon et al., 2014; Reynolds et al., 2004). This sensitivity is found to carry over to the network structure as well. The network structure of US-Wkg becomes fully connected (network type 4) in September 2014 with above average precipitation (NOAA) (Fig. 6d). ~~The relevance of climatic conditions in controlling biosphere–atmosphere interactions on three monthly time windows thus shows also on ecosystemlevel as they are strong enough to explain deviations from~~ Summarising, climatic extremes are visible in an ecosystem's trajectory as strong deviations from the median trajectory. With this finding we have to reject our second hypothesis that owing to an ecosystem's ~~median trajectory and lead to the detection of climatic extremes~~adaptation its accessible functional states are limited to a certain

range. The opposite seems to be valid. Biosphere–atmosphere interactions can follow flexibly atmospheric conditions and are not confined to certain states.

3.5 Functional convergence of biosphere–atmosphere interactions

We have seen that networks representing biosphere–atmosphere interactions ~~are strongly shaped by~~ strongly align with prevailing mean meteorological conditions. Moreover, the visualisation of ecosystem trajectories within the t-SNE space (Fig. 5, 6) and the distributions of vegetation types and climatic regions (Supplementary Material Fig. D2) reveal that ecosystems across vegetation types and climatic regions can exhibit similar biosphere–atmosphere interactions if their meteorological conditions are similar. For example, ~~at~~ we found a fully connected network (type 4) to be associated with high radiation and water availability ~~, i.e.~~ and thus optimal growing conditions, ~~ecosystems exhibit fully connected networks (type 4) as well as~~ which results in high carbon and water fluxes. Diverging from optimal growing conditions, links in the networks weaken and disappear. This behaviour can be understood as functional convergence of ecosystems which corroborates the hypothesis that ecosystems have a low number of key processes that determine ecosystem behaviour (Lambert, 2006; Meinzer, 2003; Shaver et al., 2007) rendering their behaviour transparent and predictable. Criticism might rise as the larger part of the biosphere–atmosphere interaction network indeed is a pure atmospheric network, i.e. Rg, T, VPD and H. Thus strong associations of networks and their trajectories with atmospheric conditions could be dominated by changes in this atmospheric network. Fig. 2, however, suggests the opposite. The strongest gradients are given by the links NEE–LE and Rg–LE and transitions along the axis connecting type 2 and 3 (cf. Fig. 4) are dominated by changes in biosphere connectivity, i.e. LE and NEE.

In fact, the dominance of climatic drivers in controlling the temporal evolution of ecosystem functioning emerges also in other studies ~~(Musavi et al., 2017; Schwalm et al., 2017)~~ (Musavi et al., 2017; Schwalm et al., 2017; Kraemer et al., 2020a) as they showed that carbon fluxes are primarily controlled by climatic factors. Yet, these and others also show the role of biotic factors in shaping the responses of ecosystem processes to climatic variability. For example, Musavi et al. (2017) revealed in a global ecosystem study that species diversity and ecosystem age decrease inter annual variability of GPP. Similarly, Wagg et al. (2017) ~~discovered~~ showed biodiversity to increase long-term stability of ecosystem productivity. In regional studies Wales et al. (2020) found the stability of net primary production to be affected by the kind and severity of disturbances. Tamrakar et al. (2018) showed that seasonal carbon fluxes were more sensitive to environmental conditions in a homogeneous forest compared to a heterogeneous one. It would be of interest to investigate, to which degree the effects of biotic factors also translates to the sensitivity of the network structure.

Furthermore, extreme heat and drought events (Sippel et al., 2018) or compound events in general (Zscheischler et al., 2020) can severely disrupt ecosystem functions. The time of recovery from such disturbances is a crucial parameter in assessing ecosystem resilience. Schwalm et al. (2017) showed that the recovery time measured as the recovery in GPP is primarily influenced by climate but secondarily by biodiversity and CO_2 fertilisation. Assessing the recovery time via GPP already puts the ecosystem functioning into focus. The here presented framework, i.e. the sensitivity of an ecosystem's network structure to meteorological conditions, might be a valuable asset to study reaction time and strength to and recovery from extreme events as it not only utilises one variable but the interactions of a set of variables, thereby capturing more comprehensively an ecosystem

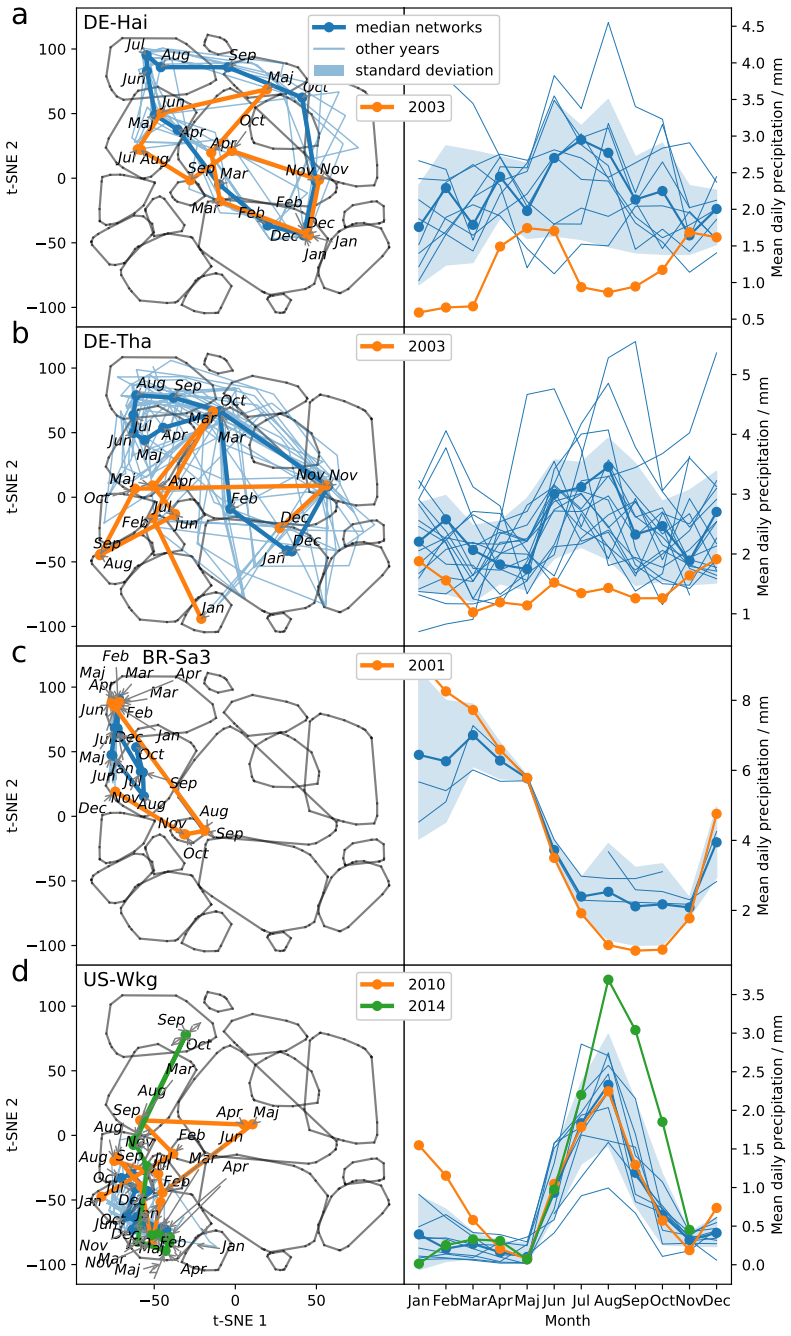

Figure 6. Abnormal conditions in meteorological conditions (here precipitation) become visible in an ecosystem's trajectory. left: Trajectories within the low dimensional space of the ecosystems Hainich (DE-Hai, DBF), Tharand (DE-Tha, ENF), Santarem-Km83-Logged Forest (BR-Sa3, EBF) and Walnut Gulch Kendall Grasslands (US-Wkg, GRA). right: Three monthly average of daily precipitation data.

state. A drawback is the reduced temporal resolution (a certain time period of daily or even half hourly measurements is aggregated to one network) which can be offset by the here used moving window approach to a certain degree. Especially with regard to climatic extreme conditions in recent years with observed vegetation dieback in, for example, DE-Hai (Schuldt et al., 2020), further studies could also shed light on the role of adaptation in shaping biosphere–atmosphere interactions. Our study suggest that adaptation to a lesser degree limits the range of possible interactions but enables to sustain and persist certain conditions for longer periods. The focus of further studies thus could be to elucidate the role of biotic factors in influencing ecosystem trajectories as well as the role of adaptation and the response to extreme events.

3.6 Limitations of the study

Finally, we would like to take a critical view on our analysis approach. As stated in Sect. 2.2, PCMCI might fail to identify some spurious links due to the occurrence of contemporaneous confounders. Thus networks can not be interpreted causally but this does not severely hinder their value for the current analysis. In addition we include a rather limited set of variables into the network estimation. Thus we cannot and do not claim that ecosystems become fully alike under similar meteorological conditions. Yet, on the timescale investigated the data shows, that the interactions among the chosen set of variables can be described by very similar structures. Follow up studies might search for and include further biosphere variables. Currently, an analysis of the biotic effects on the network structure is hampered because the t-SNE space is not metric. Thus, for instance, the effect of a drought with similar magnitude in a boreal and temperate forest cannot simply be compared by the deviation from their median trajectory.

4 Conclusions

We analysed the functional behaviour of a variety of ecosystems using the FLUXNET database of ~~eddy covariance~~ carbon, water, and energy flux measurements. In particular, we examined the interaction structure between biosphere–atmosphere fluxes as well as atmospheric state variables using PCMCI, ~~an algorithm~~ a method to estimate causal relationships from empirical time series ~~. In total we included 119 measurement sites with cumulative 1067 measurement years leading to 10038 monthly networks.~~ under certain assumptions. Using non-linear dimensionality reduction, we ~~found four~~find evidence supporting our hypothesis that the manifold of existing states is bound by few, i.e. four, archetypes of network states~~defining the edges of the low-dimensional embedding~~. They are characterised on the one hand by a fully connected and almost unconnected network structure and on the other hand by an antagonistic coupling of carbon and water flux with temperature - when one is strongly coupled, the other is decoupled. The transitions between these states correlate well with gradients of meteorological drivers, i.e. radiation and water availability. The movement of an ecosystem within that space therefore strongly aligns with changes in meteorological conditions. This, however, also leads to similar behaviour under similar conditions for strongly contrasting ecosystems. For example, forests of mid or even high latitudes exhibit similar interaction structure as tropical forests given high radiation and water availability during summer. Yet, this state can also be reached by predominantly dry ecosystems like steppe grasslands given sufficient precipitation. In contrast if productive ecosystems are struck by a severe drought, like cen-

tral European ecosystems in 2003, the behaviour can adapt more to that of a Mediterranean ecosystem. ~~Overall this~~ Thus the second part of our hypothesis must be rejected. The analysis shows that the biosphere-atmosphere interaction structure can adapt flexibly to prevailing conditions and is widely independent of vegetation type and climatic region. Such behaviour is strong evidence for functional convergence of ecosystems, i.e. their behaviour is determined by a low number of key processes. For further studies, we suggest, to focus on the role of biotic factors as, for example, plant functional types, ecosystem age and adaptation. These factors could play crucial roles in ~~copying strategies of~~ understanding the ecosystem copying strategies to climatic extremes.

Code availability. Code scripts can be found at https://github.com/ckrich/Functional-convergence-of-biosphere-atmosphere-interactions-in-response-to-meteorology

Data availability. The eddy covariance data of the FLUXNET sites can be downloaded from the official webpage (https://fluxnet.fluxdata.org/).

Appendix A: Methods

Table A1: List of FLUXNET sites used for the generation of artificial datasets and the time period used.

FLUXNET-ID	~~start year end year data reference~~ IBGP	~~FLUXNET-ID~~ Koeppen-Geiger Class	start year	end year	data referen
AT-Neu	GRA	Dfb	2002		
AU-ASM	~~IT-BCi~~ ENF	~~2004~~ BSh	2010		
~~AU-ASM~~ AU-Cpr	SAV	Csa	2010		
AU-DaP	~~IT-Col~~ GRA	~~1996~~ Aw	~~2014~~ 2007		~~Valentini e~~
~~AU-Cpr~~ AU-DaS	~~2010~~ SAV	Aw	2008		
AU-Dry	~~IT-Cpz~~ SAV	~~1997~~	~~2009~~ 2008		~~Garbulsky~~
~~AU-DaP~~ AU-How	~~2007~~ WSA	~~2013~~ Aw	~~Beringer et al. (2011a)~~ 2001		~~IT-~~
AU-Stp	GRA	Aw	2008		
~~AU-DaS~~ AU-Tum	~~2008~~ EBF	Cfb	2001		
AU-Wom	~~IT-MBo~~ EBF	~~2003~~ Cfb	~~2013~~ 2010		~~Marcolla e~~
~~AU-Dry~~ BE-Bra	~~2008~~ MF	Cfb	1996		
BE-Lon	~~IT-Noe~~ CRO	BSk	2004		
~~AU-How~~ BE-Vie	~~2001~~ MF	Cfb	1996		
BR-Sa3	~~IT-Non~~ EBF		2000		
CA-Mer	WET	Dwb	1998		

Continued on next pa

Table A1 – *Continued from previous pa*

FLUXNET-ID	start year end year data reference IBGP	FLUXNET-ID Koeppen-Geiger Class	start year	end year	data referen
CA-NS1	ENF	BWk	2001		20
AU-Stp CA-NS2	2008 ENF	2014 BWk	Beringer et al. (2011b) 2001		IT-
CA-NS3	2013 ENF	Marcolla et al. (2005)	2001		
AU-Tum CA-NS5	ENF	BSk	2001		20
CA-NS6	IT-Ro1 OSH	2000 BSk	2008 2001		Rey et a
AU-Wom CA-Qcu	ENF	Dwb	2001		
CA-Qfo	ENF	Dfb	2003		
CA-SF2	Arndt et al. ENF	IT-Ro2 BSk	2002 2001		20
BE-Bra CA-SF3	1996 OSH	2014 Dwc	Carrara et al. (2004) 2001		IT-
CH-Cha	2012 GRA	Chiesi et al. (2005) Cfb	2005		
BE-Lon CH-Dav	2004 ENF	Dfc	1997		
CH-Fru	IT-Tor GRA	2008 Dfb	2005		
BE-Vie CH-Lae	1996 MF	BWk	2004		
CH-Oe1	JP-SMF GRA	Cfb	2002		20
BR-Sa3 CH-Oe2	2000 CRO	BSk	2004		Saleska et
CZ-BK1	ENF	Dwb	2004		20
CA-Mer CZ-BK2	1998 GRA	2005 Dfb	Lafleur et al. (2003) 2004		NL-
CZ-wet	WET	Dfb	2006		
CA-NS1 DE-Akm	2001 WET	2005 BWk	Goulden et al. (2006) 2009		PT-
DE-Geb	2006 CRO	Rodrigues et al. (2011) CA-NS2 Cfb	2001		20
DE-Gri	RU-Cok GRA	2003 Dfb	2004		
CA-NS3 DE-Hai	2001 DBF	2005 Cfb	Wang et al. (2002a) 2000		RU-
DE-Kli	2014 CRO	Kurbatova et al. (2008) CA-NS5 Dfb	2001 2004		20
DE-Lkb	SD-Dem ENF	2005 Dwb	2009		Ardö et a
CA-NS6 DE-Obe	2001 ENF	2005 Dfb	Wang et al. (2002c) 2008		SE-
DE-Spw	2005 WET	Sagerfors et al. (2008) CA-Qcu BWk	2001 2010		
DE-Tha	SE-Fla ENF	Dfb	1996		
DE-Wet	ENF	Dfb	2002		Valer
CA-Qfo DK-NuF	2003 WET	2010 Dfc	Chen et al. (2006) 2008		
DK-Sor	DBF	Cfb	1996		
CA-SF2 DK-ZaH	2001 GRA	2005 ET	Rayment and Jarvis (1999a) 2000		
ES-ES1	ENF	BSk	1999		

Continued on next pa

Table A1 – *Continued from previous pa*

FLUXNET-ID	start year end year data reference IBGP	FLUXNET-ID Koeppen-Geiger Class	start year	end year	data referen
CA-SF3 FI-Hyy	2001 ENF	2006 Dfb	Rayment and Jarvis (1999b) 1996		
FI-Kaa	2012 WET	Fischer et al. (2007) Dfc	2000		
CH-Cha FI-Sod	2005 ENF	BSk	2001		
FR-Fon	US-Aud DBF	2002 Cfb	2006 2005		
CH-Dav FR-Gri	1997 CRO	Cfb	2004		
FR-Hes	US-Blo DBF	Cfb	1997		
CH-Fru FR-LBr	2005 ENF	2014 Cfb	Imer et al. (2013) 1996		
FR-Pue	2007 EBF	Meyers and Hollinger (2004) Csa	2000		
CH-Lae GF-Guy	EBF	Am	2004		
HU-Bug	US-Cop GRA	2001 Dfb	2007 2002		Rue
CH-Oe1 IL-Yat	2002 ENF	2008 BWh	Ammann et al. (2009) 2001		
IT-Amp	GRA	Dsb	2002		
CH-Oe2 IT-BCi	CRO	Csa	2004		
IT-Col	US-GBT DBF	1999 Dsb	2006 1996		Zel
CZ-BK1 IT-Cpz	2004 EBF	2014 Csa	Acosta et al. (2013) 1997		
IT-Lav	ENF	Dwb	2003		
CZ-BK2 IT-MBo	2004 GRA	2012 Dfb	–2003		
IT-Noe	2012 CSH	Wofsy et al. (1993) CZ-wet BSk	2006 2004		
IT-Non	US-Ho1 DBF	1996 Cfa	2004 2001		Arms
DE-Akm IT-Ren	2009 ENF	2014 BSk	–1998		
IT-Ro1	DBF	Csa	2000		
DE-Geb IT-Ro2	2001 DBF	2014 Csa	Anthoni et al. (2004b) 2002		
IT-SRo	ENF	BSk	1999		
DE-Gri IT-Tor	2004 GRA	BSk	2008		
JP-SMF	US-Me2 MF	Cfa	2002		
DE-Hai NL-Hor	2000 GRA	2012 Csb	Knohl et al. (2003) 2004		
NL-Loo	2014 ENF	Ruehr et al. (2012b) DE-Kli Cfb	2004 1996		
PT-Esp	US-Myb EBF	2010 Csa	2014 2002		R
DE-Lkb RU-Cok	2009 OSH	2013 Dwd	Lindauer et al. (2014) 2003		
RU-Fyo	ENF	Dwb	1998		
DE-Obe SD-Dem	2008 SAV	2014 BWh	–2005		
SE-Deg	WET	Dwc	2001		

Continued on next pa

Table A1 – *Continued from previous pa*

FLUXNET-ID	start year end year data reference IBGP	FLUXNET-ID Koeppen-Geiger Class	start year	end year	data referen
DE-Spw SE-Fla	2010 ENF	2014 Dwc	– 1996		
SE-Nor	2013 EBF	Cassman et al. (2003a) DE-Tha BSk	1996		
UK-Gri	US-Ne3 ENF	2001 Csb	2013 1997		
DE-Wet US-ARM	CRO	Csa	2003		
US-Aud	GRA	BSk	2002		
US-Blo	US-PFa ENF	1995 Csb	2014 1997		
DK-NuF US-Bo1	2008 CRO	2014 Dfa	Westergaard-Nielsen et al. (2013) 1996		
US-Cop	2014 GRA	Ruehr et al. (2012d) DK-Sor BWk	1996 2001		
US-FPe	US-SP1 GRA	BSk	2000		
DK-ZaH US-GBT	2000 ENF	2014 BWk	Lund et al. (2012) 1999		
US-GLE	ENF	Dsc	2004		
ES-ES1 US-Ha1	1999 DBF	2006 Dfb	Sanz et al. (2004) 1991		
US-Ho1	ENF	Dfb	1996		
FI-Hyy US-Los	1996 WET	Dfb	2000		
US-MMS	US-SRG DBF	2008 Dfa	1999		
FI-Kaa US-Me2	2000 ENF	2006 Dsb	Aurela et al. (2007) 2002		
US-Me6	ENF	BSk	2010		
FI-Sod US-Myb	2001 WET	Csb	2010		
US-NR1	US-Syv ENF	2001 Dfc	1998		
FR-Fon US-Ne1	2005 CRO	2014 Dwa	Delpierre et al. (2016) 2001		
US-Ne2	CRO	Dwa	2001		
FR-Gri US-Ne3	2004 CRO	2014 Dwa	Loubet et al. (2011) 2001		
US-PFa	MF	Dwb	1995		
FR-Hes US-Prr	1997 ENF	2006 Dwc	Granier et al. (2000) 2010		
US-SP1	ENF	BWh	2000		
FR-LBr US-SP2	1996 ENF	2008 Csa	Berbigier et al. (2001) 1998		
US-SP3	ENF	Csa	1999		
US-SRG	GRA	BSh	2008		
FR-Pue US-SRM	2000 WSA	BSh	2004		
US-Syv	US-Var MF	2000 Dfb	2001		
GF-Guy US-Ton	2004 WSA	Csa	2001		
US-Twt	US-WCr CRO	1999 Csb	2009		

Continued on next pa

Table A1 – *Continued from previous pa*

FLUXNET-ID	start year end year data reference IBGP	FLUXNET-ID Koeppen-Geiger Class	start year	end year	data referen
HU-Bug US-UMB	2002 DBF	2006 Dfb	Nagy et al. (2005) 2000		
US-UMd	DBF	BWk	2007		
IL-Yat US-Var	2001 GRA	2006 Csa	Grünzweig et al. (2003) 2000		
US-WCr	DBF	Dfb	1999		
IT-Amp US-Whs	2002 OSH	2006 BWk	Gilmanov et al. (2007) 2007		
US-Wkg	2013 GRA	Archibald et al. (2009) IT-BCi BWk	2004		
ZA-Kru	SAV	BSh	2000		
ZM-Mon	DBF	Aw	2000		

Table B1. PCMCI parameters that were used differently from default settings.

PCMCI parameter	Setting
significance α	0.1
α_{pc}	None
tau_min	0
tau_max	5
~~selected_variables T, NEE, VPD, H, LE~~mask_type	'y'
fdr_method	'fdr_bh'
selected_links (for variable set [R_g, T, NEE, VPD, H, LE])	{0: [], for i in [1,2,3,4,5]: i:[(i,-1), (i,-2)] + [(j,0), (j,-1), (j,-2) for j in [1,2,3,4,5] and j≠i]}

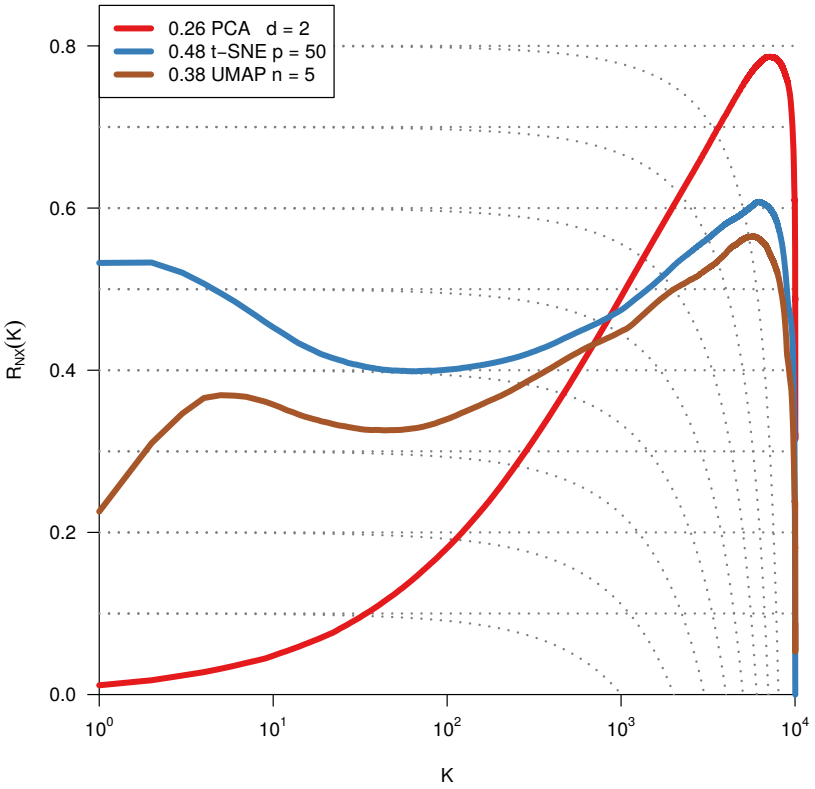

Figure A1. Quality assessment of dimensionality reduction techniques. To visualize and subsequently analyse the network space we reduce its dimensionality. We compared PCA, t-SNE and UMAP including various parameter settings (here: PCA's leading two principal components, t-SNE with perplexity 30, and UMAP with $n_{neighbors}$ equal 5 for 2 dimensions). The test statistic $R_{NX}(k)$ (y-axis) gives the improvement of the embedding of k-neighborhoods (x-axis) over a random embedding. The area under the curves (preserving the log-scaled x-axis) is given in the legend and gives an idea of the overall quality of the embedding Lee et al. (2015). We chose t-SNE with perplexity 30, as it preserves best local neighbourhoods and performs well on larger distances.

Appendix C: Results and Discussion

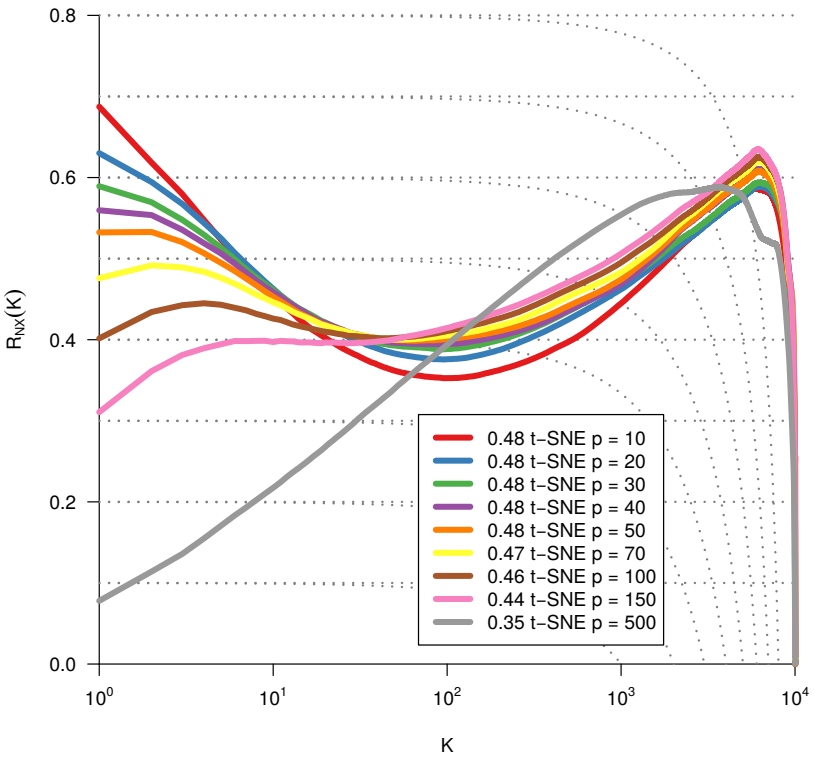

Figure B1. Same metric as Fig. A1. Optimisation of the dimensionality reduction via t-SNE by using different perplexity values.

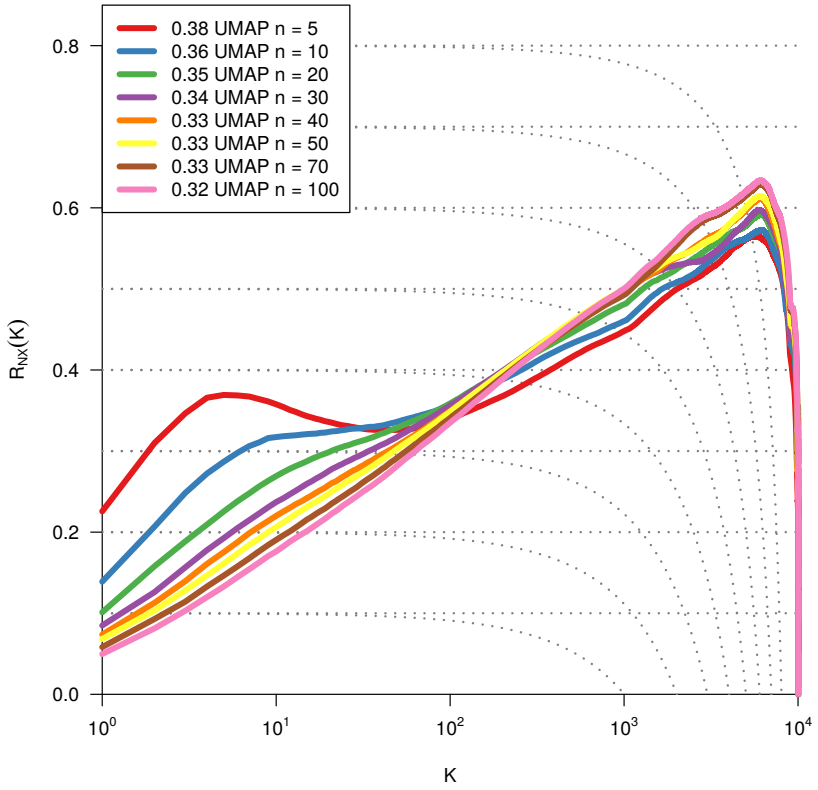

Figure C1. Same metric as Fig. A1. Optimisation of the dimensionality reduction to two dimensions via UMAP by using different values for the parameter $n_{neighbors}$.

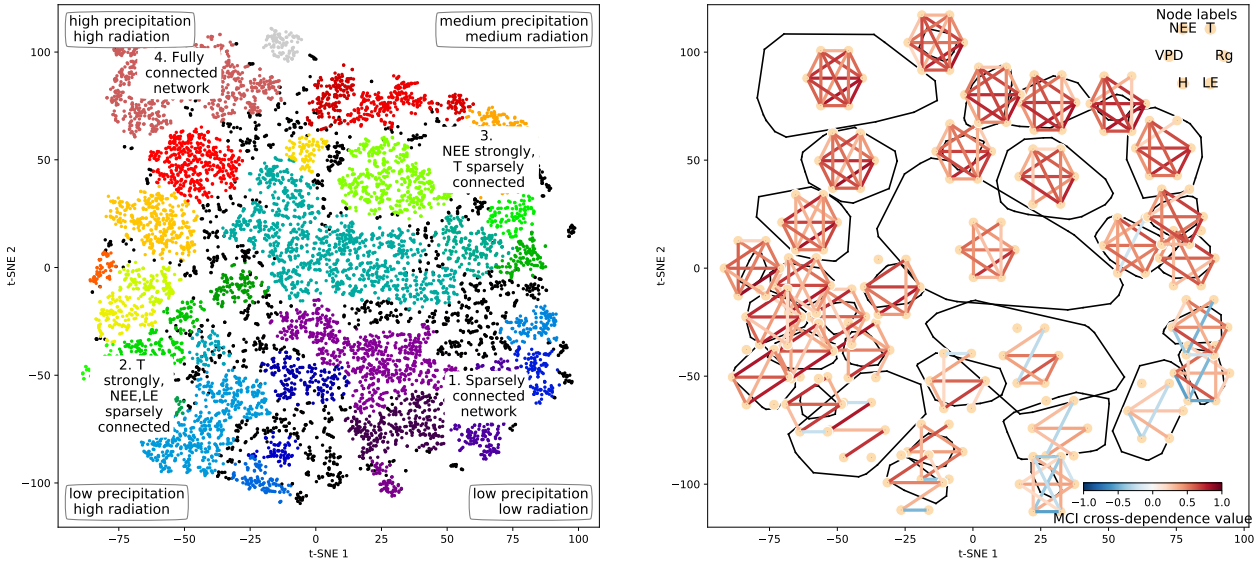

Figure D1. As Fig. 4 but with smaller clusters exhibiting the finer structure of the t-SNE space.

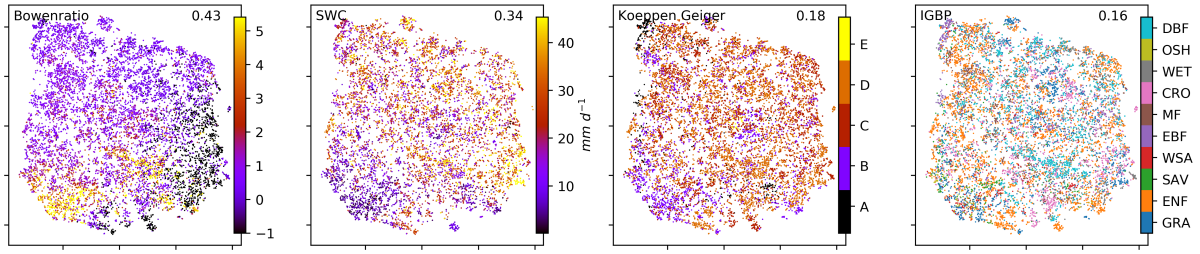

Figure D2. t-SNE space coloured by underlying mean Bowenratio and precipitation, as well as the ecosystems respective Koeppen Geiger class and IGBP type.

Author contributions. CK and MDM designed the study with contributions from all other authors. CK conducted the analysis and wrote the manuscript. All authors helped to improve the manuscript.

Competing interests. The authors declare that they have no competing financial interests.

Acknowledgements. D.G.M. acknowledges support from the European Research Council under grant agreement number 715254 (DRY-2-DRY). CK thanks the Max Planck Research School for global Biogeochemical Cycles for supporting his PhD project as well as Jacob A. Nelson in helping to assemble the dataset. This work used eddy covariance data acquired and shared by the FLUXNET community, including these networks: AmeriFlux, AfriFlux, AsiaFlux, CarboAfrica, CarboEuropeIP, CarboItaly, CarboMont, ChinaFlux, Fluxnet-Canada, GreenGrass, ICOS, KoFlux, LBA, NECC, OzFlux-TERN, TCOS-Siberia, and USCCC. The ERA-Interim reanalysis data are provided by ECMWF and processed by LSCE. The FLUXNET eddy covariance data processing and harmonization was carried out by the European Fluxes Database Cluster, AmeriFlux Management Project, and Fluxdata project of FLUXNET, with the support of CDIAC and ICOS Ecosystem Thematic Center, and the OzFlux, ChinaFlux and AsiaFlux offices.

References

Acosta, M., Pavelka, M., Montagnani, L., Kutsch, W., Lindroth, A., Juszczak, R., and Janouš, D.: Soil Surface CO2 Efflux Measurements in Norway Spruce Forests: Comparison between Four Different Sites across Europe — from Boreal to Alpine Forest, Geoderma, 192, 295–303, https://doi.org/10.1016/j.geoderma.2012.08.027, 2013.

Ammann, C., Spirig, C., Leifeld, J., and Neftel, A.: Assessment of the Nitrogen and Carbon Budget of Two Managed Temperate Grassland Fields, Agriculture, Ecosystems & Environment, 133, 150–162, https://doi.org/10.1016/j.agee.2009.05.006, 2009.

Ankerst, M., Breunig, M. M., Kriegel, H.-P., and Sander, J.: OPTICS: ordering points to identify the clustering structure, ACM Sigmod record, 28, 49–60, 1999.

Anthoni, P., Knohl, A., Rebmann, C., Freibauer, A., Mund, M., Ziegler, W., Kolle, O., and Schulze, E.-D.: Forest and agricultural land-use-dependent CO2 exchange in Thuringia, Germany, Global Change Biology, 10, 2005–2019, 2004a.

Anthoni, P. M., Knohl, A., Rebmann, C., Freibauer, A., Mund, M., Ziegler, W., Kolle, O., and Schulze, E.-D.: Forest and Agricultural Land-Use-Dependent CO2 Exchange in Thuringia, Germany, Global Change Biology, 10, 2005–2019, https://doi.org/10.1111/j.1365-2486.2004.00863.x, 2004b.

Archibald, S. A., Kirton, A., van der Merwe, M. R., Scholes, R. J., Williams, C. A., and Hanan, N.: Drivers of Inter-Annual Variability in Net Ecosystem Exchange in a Semi-Arid Savanna Ecosystem, South Africa, Biogeosciences, 6, 251–266, https://doi.org/https://doi.org/10.5194/bg-6-251-2009, 2009.

Ardö, J., Mölder, M., El-Tahir, B. A., and Elkhidir, H. A. M.: Seasonal Variation of Carbon Fluxes in a Sparse Savanna in Semi Arid Sudan, Carbon Balance and Management, 3, 7, https://doi.org/10.1186/1750-0680-3-7, 2008.

Armstrong, N. and Ernst, E.: The treatment of eczema with Chinese herbs: a systematic review of randomized clinical trials, British journal of clinical pharmacology, 48, 262, 1999.

Arndt, S., Hinko-Najera, N., Griebel, A., Beringer, J., and Livesley, S. J.: FLUXNET2015 AU-Wom Wombat, https://doi.org/10.18140/FLX/1440207.

Aubinet, M., Chermanne, B., Vandenhaute, M., Longdoz, B., Yernaux, M., and Laitat, E.: Long Term Carbon Dioxide Exchange above a Mixed Forest in the Belgian Ardennes, Agricultural and Forest Meteorology, 108, 293–315, https://doi.org/https://doi.org/10.1016/S0168-1923(01)00244-1, 2001.

Aubinet, M., Vesala, T., and Papale, D.: Eddy covariance: a practical guide to measurement and data analysis, Springer Science & Business Media, 2012.

Aurela, M., Riutta, T., Laurila, T., Tuovinen, J.-P., Vesala, T., Tuittila, E.-S., Rinne, J., Haapanala, S., and Laine, J.: CO2 exchange of a sedge fen in southern Finland-The impact of a drought period, Tellus B: Chemical and Physical Meteorology, 59, 826–837, 2007.

Baker, I., Denning, A. S., Hanan, N., Prihodko, L., Uliasz, M., Vidale, P.-L., Davis, K., and Bakwin, P.: Simulated and Observed Fluxes of Sensible and Latent Heat and CO2 at the WLEF-TV Tower Using SiB2.5, Global Change Biology, 9, 1262–1277, https://doi.org/10.1046/j.1365-2486.2003.00671.x, 2003.

Baldocchi, D.: 'Breathing'of the terrestrial biosphere: lessons learned from a global network of carbon dioxide flux measurement systems, Australian Journal of Botany, 56, 1–26, 2008.

Baldocchi, D.: Measuring fluxes of trace gases and energy between ecosystems and the atmosphere – the state and future of the eddy covariance method, Global Change Biology, 20, 3600–3609, https://doi.org/10.1111/gcb.12649, http://dx.doi.org/10.1111/gcb.12649, 2014.

Baldocchi, D., Falge, E., Gu, L., Olson, R., Hollinger, D., Running, S., Anthoni, P., Bernhofer, C., Davis, K., Evans, R., Fuentes, J., Goldstein, A., Katul, G., Law, B., Lee, X., Malhi, Y., Meyers, T., Munger, W., Oechel, W., Paw U, K. T., Pilegaard, K., Schmid, H. P., Valentini, R., Verma, S., Vesala, T., Wilson, K., and Wofsy, S.: FLUXNET: A New Tool to Study the Temporal and Spatial Variability of Ecosystem-Scale Carbon Dioxide, Water Vapor, and Energy Flux Densities, Bulletin of the American Meteorological Society, 82, 2415–2434, https://doi.org/10.1175/1520-0477(2001)082<2415:FANTTS>2.3.CO;2, https://doi.org/10.1175/1520-0477(2001)082<2415:FANTTS>2.3.CO;2, 2001.

Baldocchi, D., Ryu, Y., and Keenan, T.: Terrestrial Carbon Cycle Variability [version 1; peer review: 2 approved, F1000Research, 5(F1000 Faculty Rev), https://doi.org/(https://doi.org/10.12688/f1000research.8962.1), 2016.

Beer, C., Reichstein, M., Tomelleri, E., Ciais, P., Jung, M., Carvalhais, N., Rödenbeck, C., Arain, M. A., Baldocchi, D., Bonan, G. B., Bondeau, A., Cescatti, A., Lasslop, G., Lindroth, A., Lomas, M., Luyssaert, S., Margolis, H., Oleson, K. W., Roupsard, O., Veenendaal, E., Viovy, N., Williams, C., Woodward, F. I., and Papale, D.: Terrestrial Gross Carbon Dioxide Uptake: Global Distribution and Covariation with Climate, Science, 329, 834–838, https://doi.org/10.1126/science.1184984, http://science.sciencemag.org/content/329/5993/834, 2010.

Berbigier, P., Bonnefond, J.-M., and Mellmann, P.: CO2 and Water Vapour Fluxes for 2 Years above Euroflux Forest Site, Agricultural and Forest Meteorology, 108, 183–197, https://doi.org/10.1016/S0168-1923(01)00240-4, 2001.

Beringer, J., Hutley, L. B., Tapper, N. J., and Cernusak, L. A.: Savanna Fires and Their Impact on Net Ecosystem Productivity in North Australia, Global Change Biology, 13, {990–1004}, https://doi.org/{10.1111/j.1365-2486.2007.01334.x}, 2007.

Beringer, J., Hutley, L. B., Hacker, J. M., Neininger, B., and U, K. T. P.: Patterns and Processes of Carbon, Water and Energy Cycles across Northern Australian Landscapes: From Point to Region, Agricultural and Forest Meteorology, 151, {1409–1416}, https://doi.org/{10.1016/j.agrformet.2011.05.003}, 2011a.

Beringer, J., Hutley, L. B., Hacker, J. M., Neininger, B., and U, K. T. P.: Patterns and Processes of Carbon, Water and Energy Cycles across Northern Australian Landscapes: From Point to Region, Agricultural and Forest Meteorology, 151, 1409–1416, https://doi.org/https://doi.org/10.1016/j.agrformet.2011.05.003, savanna Patterns of Energy and Carbon Integrated Across the Landscape (SPECIAL), 2011b.

Bernhofer, C., Grünwald, T., Moderow, U., Hehn, M., Eichelmann, U., Prasse, H., and Postel, U.: FLUXNET2015 DE-Akm Anklam, https://doi.org/10.18140/FLX/1440213, a.

Bernhofer, C., Grünwald, T., Moderow, U., Hehn, M., Eichelmann, U., Prasse, H., and Postel, U.: FLUXNET2015 DE-Obe Oberbärenburg, https://doi.org/10.18140/FLX/1440151, b.

Bernhofer, C., Grünwald, T., Moderow, U., Hehn, M., Eichelmann, U., Prasse, H., and Postel, U.: FLUXNET2015 DE-Spw Spreewald, https://doi.org/10.18140/FLX/1440220, c.

Bonal, D., Bosc, A., Ponton, S., Goret, J.-Y., Burban, B., Gross, P., Bonnefond, J.-M., Elbers, J., Longdoz, B., Epron, D., Guehl, J.-M., and Granier, A.: Impact of Severe Dry Season on Net Ecosystem Exchange in the Neotropical Rainforest of French Guiana, Global Change Biology, 14, 1917–1933, https://doi.org/10.1111/j.1365-2486.2008.01610.x, 2008.

Bonan, G.: Ecological Climatology: Concepts and Applications, Cambridge University Press, 3 edn., https://doi.org/10.1017/CBO9781107339200, 2015.

Bond-Lamberty, B., Wang, C., and Gower, S. T.: Net Primary Production and Net Ecosystem Production of a Boreal Black Spruce Wildfire Chronosequence, Global Change Biology, 10, 473–487, https://doi.org/10.1111/j.1529-8817.2003.0742.x, 2004.

Carrara, A., Janssens, I. A., Yuste, J. C., and Ceulemans, R.: Seasonal Changes in Photosynthesis, Respiration and NEE of a Mixed Temperate Forest, Agricultural and Forest Meteorology, 126, 15–31, https://doi.org/https://doi.org/10.1016/j.agrformet.2004.05.002, 2004.

Cassman, K. G., Dobermann, A., Walters, D. T., and Yang, H.: Meeting Cereal Demand While Protecting Natural Resources and Improving Environmental Quality, Annual Review of Environment and Resources, 28, 315–358, https://doi.org/10.1146/annurev.energy.28.040202.122858, 2003a.

Cassman, K. G., Dobermann, A., Walters, D. T., and Yang, H.: Meeting Cereal Demand While Protecting Natural Resources and Improving Environmental Quality, Annual Review of Environment and Resources, 28, 315–358, https://doi.org/10.1146/annurev.energy.28.040202.122858, 2003b.

Cernusak, L. A., Hutley, L. B., Beringer, J., Holtum, J. A. M., and Turner, B. L.: Photosynthetic Physiology of Eucalypts along a Sub-Continental Rainfall Gradient in Northern Australia, Agricultural and Forest Meteorology, 151, {1462–1470}, https://doi.org/{10.1016/j.agrformet.2011.01.006}, 2011.

Chen, J. M., Govind, A., Sonnentag, O., Zhang, Y., Barr, A., and Amiro, B.: Leaf Area Index Measurements at Fluxnet-Canada Forest Sites, Agricultural and Forest Meteorology, 140, 257–268, https://doi.org/10.1016/j.agrformet.2006.08.005, 2006.

Chiesi, M., Maselli, F., Bindi, M., Fibbi, L., Cherubini, P., Arlotta, E., Tirone, G., Matteucci, G., and Seufert, G.: Modelling Carbon Budget of Mediterranean Forests Using Ground and Remote Sensing Measurements, Agricultural and Forest Meteorology, 135, 22–34, https://doi.org/10.1016/j.agrformet.2005.09.011, 2005.

Claessen, J., Molini, A., Martens, B., Detto, M., Demuzere, M., and Miralles, D.: Global biosphere–climate interaction: a multi-scale appraisal of observations and models, Biogeosciences Discussions, 2019, 1–30, https://doi.org/10.5194/bg-2019-212, https://www.biogeosciences-discuss.net/bg-2019-212/, 2019.

Cleverly, J., Boulain, N., Villalobos-Vega, R., Grant, N., Faux, R., Wood, C., Cook, P. G., Yu, Q., Leigh, A., and Eamus, D.: Dynamics of Component Carbon Fluxes in a Semi-Arid Acacia Woodland, Central Australia, Journal of Geophysical Research: Biogeosciences, 118, {1168–1185}, https://doi.org/{10.1002/jgrg.20101}, 2013.

Delpierre, N., Berveiller, D., Granda, E., and Dufrêne, E.: Wood Phenology, Not Carbon Input, Controls the Interannual Variability of Wood Growth in a Temperate Oak Forest, New Phytologist, 210, 459–470, https://doi.org/10.1111/nph.13771, 2016.

Desai, A. R., Bolstad, P. V., Cook, B. D., Davis, K. J., and Carey, E. V.: Comparing Net Ecosystem Exchange of Carbon Dioxide between an Old-Growth and Mature Forest in the Upper Midwest, USA, Agricultural and Forest Meteorology, 128, 33–55, https://doi.org/10.1016/j.agrformet.2004.09.005, 2005.

Detto, M., Molini, A., Katul, G., Stoy, P., Palmroth, S., and Baldocchi, D.: Causality and Persistence in Ecological Systems: A Nonparametric Spectral Granger Causality Approach., The American Naturalist, 179, 524–535, https://doi.org/10.1086/664628, https://doi.org/10.1086/664628, pMID: 22437181, 2012.

Dietiker, D., Buchmann, N., and Eugster, W.: Testing the Ability of the DNDC Model to Predict CO2 and Water Vapour Fluxes of a Swiss Cropland Site, Agriculture, Ecosystems & Environment, 139, 396–401, https://doi.org/10.1016/j.agee.2010.09.002, 2010.

Dušek, J., Čížková, H., Stellner, S., Czerný, R., and Květ, J.: Fluctuating Water Table Affects Gross Ecosystem Production and Gross Radiation Use Efficiency in a Sedge-Grass Marsh, Hydrobiologia, 692, 57–66, https://doi.org/10.1007/s10750-012-0998-z, 2012.

Emmerich, W. E.: Carbon Dioxide Fluxes in a Semiarid Environment with High Carbonate Soils, Agricultural and Forest Meteorology, 116, 91–102, https://doi.org/10.1016/S0168-1923(02)00231-9, 2003.

Etzold, S., Ruehr, N. K., Zweifel, R., Dobbertin, M., Zingg, A., Pluess, P., Häsler, R., Eugster, W., and Buchmann, N.: The Carbon Balance of Two Contrasting Mountain Forest Ecosystems in Switzerland: Similar Annual Trends, but Seasonal Differences, Ecosystems, 14, 1289–1309, https://doi.org/10.1007/s10021-011-9481-3, 2011.

Fischer, M. L., Billesbach, D. P., Berry, J. A., Riley, W. J., and Torn, M. S.: Spatiotemporal Variations in Growing Season Exchanges of CO2, H2O, and Sensible Heat in Agricultural Fields of the Southern Great Plains, Earth Interactions, 11, 1–21, https://doi.org/10.1175/EI231.1, 2007.

Flach, M., Sippel, S., Gans, F., Bastos, A., Brenning, A., Reichstein, M., and Mahecha, M. D.: Contrasting biosphere responses to hydrometeorological extremes: revisiting the 2010 western Russian heatwave, Biogeosciences, 15, 6067–6085, https://doi.org/10.5194/bg-15-6067-2018, https://www.biogeosciences.net/15/6067/2018/, 2018.

Galvagno, M., Wohlfahrt, G., Cremonese, E., Rossini, M., Colombo, R., Filippa, G., Julitta, T., Manca, G., Siniscalco, C., di Cella, U. M., and Migliavacca, M.: Phenology and Carbon Dioxide Source/Sink Strength of a Subalpine Grassland in Response to an Exceptionally Short Snow Season, Environmental Research Letters, 8, 025 008, https://doi.org/10.1088/1748-9326/8/2/025008, 2013.

Garbulsky, M. F., Peñuelas, J., Papale, D., and Filella, I.: Remote Estimation of Carbon Dioxide Uptake by a Mediterranean Forest, Global Change Biology, 14, 2860–2867, https://doi.org/10.1111/j.1365-2486.2008.01684.x, 2008.

Giasson, M.-A., Coursolle, C., and Margolis, H. A.: Ecosystem-level CO2 fluxes from a boreal cutover in eastern Canada before and after scarification, Agricultural and Forest Meteorology, 140, 23–40, 2006.

Gilmanov, T., Soussana, J.-F., Aires, L., Allard, V., Ammann, C., Balzarolo, M., Barcza, Z., Bernhofer, C., Campbell, C., Cernusca, A., et al.: Partitioning European grassland net ecosystem CO2 exchange into gross primary productivity and ecosystem respiration using light response function analysis, Agriculture, ecosystems & environment, 121, 93–120, 2007.

Gilmanov, T. G., Tieszen, L. L., Wylie, B. K., Flanagan, L. B., Frank, A. B., Haferkamp, M. R., Meyers, T. P., and Morgan, J. A.: Integration of CO2 flux and remotely-sensed data for primary production and ecosystem respiration analyses in the Northern Great Plains: Potential for quantitative spatial extrapolation, Global Ecology and Biogeography, 14, 271–292, 2005.

Gitelson, A. A., Viña, A., Arkebauer, T. J., Rundquist, D. C., Keydan, G., and Leavitt, B.: Remote Estimation of Leaf Area Index and Green Leaf Biomass in Maize Canopies, Geophysical Research Letters, 30, https://doi.org/10.1029/2002GL016450, 2003.

Goodwell, A. E. and Kumar, P.: Temporal Information Partitioning Networks (TIPNets): A process network approach to infer ecohydrologic shifts, Water Resources Research, 53, 5899–5919, https://doi.org/10.1002/2016WR020218, https://agupubs.onlinelibrary.wiley.com/doi/abs/10.1002/2016WR020218, 2017.

Goulden, M. L., Winston, G. C., McMILLAN, A. M. S., Litvak, M. E., Read, E. L., Rocha, A. V., and Elliot, J. R.: An Eddy Covariance Mesonet to Measure the Effect of Forest Age on Land–Atmosphere Exchange, Global Change Biology, 12, 2146–2162, https://doi.org/10.1111/j.1365-2486.2006.01251.x, 2006.

Granger, C. W. J.: Investigating Causal Relations by Econometric Models and Cross-spectral Methods, Econometrica, 37, 424–438, http://www.jstor.org/stable/1912791, 1969.

Granier, A., Ceschia, E., Damesin, C., Dufrêne, E., Epron, D., Gross, P., Lebaube, S., Le Dantec, V., Le Goff, N., Lemoine, D., et al.: The carbon balance of a young beech forest, Functional ecology, 14, 312–325, 2000.

Green, J., G. Konings, A., Alemohammad, S. H., Berry, J., Entekhabi, D., Kolassa, J., Lee, J.-E., and Gentine, P.: Regionally strong feedbacks between the atmosphere and terrestrial biosphere, NATURE GEOSCIENCE, 10, 410–414, https://doi.org/http://dx.doi.org/10.1038/ngeo2957, https://www.nature.com/ngeo/journal/v10/n6/pdf/ngeo2957.pdf, 2017.

Grünwald, T. and Bernhofer, C.: A Decade of Carbon, Water and Energy Flux Measurements of an Old Spruce Forest at the Anchor Station Tharandt, Tellus B: Chemical and Physical Meteorology, 59, 387–396, https://doi.org/10.1111/j.1600-0889.2007.00259.x, 2007.

Grünzweig, J., Lin, T., Rotenberg, E., Schwartz, A., and Yakir, D.: Carbon sequestration in arid-land forest, Global Change Biology, 9, 791–799, 2003.

Hatala, J. A., Detto, M., and Baldocchi, D. D.: Gross Ecosystem Photosynthesis Causes a Diurnal Pattern in Methane Emission from Rice, Geophysical Research Letters, 39, https://doi.org/10.1029/2012GL051303, 2012.

Hutley, L. B., Beringer, J., Isaac, P. R., Hacker, J. M., and Cernusak, L. A.: A Sub-Continental Scale Living Laboratory: Spatial Patterns of Savanna Vegetation over a Rainfall Gradient in Northern Australia, Agricultural and Forest Meteorology, 151, {1417–1428}, https://doi.org/{10.1016/j.agrformet.2011.03.002}, 2011.

Imer, D., Merbold, L., Eugster, W., and Buchmann, N.: Temporal and Spatial Variations of Soil CO_2, CH_4 and N_2O Fluxes at Three Differently Managed Grasslands, Biogeosciences, 10, 5931–5945, https://doi.org/https://doi.org/10.5194/bg-10-5931-2013, 2013.

Jacobs, C. M. J., Jacobs, A. F. G., Bosveld, F. C., Hendriks, D. M. D., Hensen, A., Kroon, P. S., Moors, E. J., Nol, L., Schrier-Uijl, A., and Veenendaal, E. M.: Variability of Annual CO_2 Exchange from Dutch Grasslands, Biogeosciences, 4, 803–816, https://doi.org/https://doi.org/10.5194/bg-4-803-2007, 2007.

Knohl, A., Schulze, E.-D., Kolle, O., and Buchmann, N.: Large Carbon Uptake by an Unmanaged 250-Year-Old Deciduous Forest in Central Germany, Agricultural and Forest Meteorology, 118, 151–167, https://doi.org/10.1016/S0168-1923(03)00115-1, 2003.

Kobak, D. and Linderman, G. C.: UMAP does not preserve global structure any better than t-SNE when using the same initialization, bioRxiv, https://doi.org/10.1101/2019.12.19.877522, https://www.biorxiv.org/content/early/2019/12/19/2019.12.19.877522, 2019.

Kraemer, G., Camps-Valls, G., Reichstein, M., and Mahecha, M. D.: Summarizing the state of the terrestrial biosphere in few dimensions, Biogeosciences, 17, 2397–2424, 2020a.

Kraemer, G., Reichstein, M., Camps-Valls, G., Smits, J., and Mahecha, M. D.: The Low Dimensionality of Development, Social Indicators Research, pp. 1–22, 2020b.

Krich, C., Runge, J., Miralles, D. G., Migliavacca, M., Perez-Priego, O., El-Madany, T., Carrara, A., and Mahecha, M. D.: Estimating causal networks in biosphere–atmosphere interaction with the PCMCI approach, Biogeosciences, 17, 1033–1061, https://doi.org/10.5194/bg-17-1033-2020, https://www.biogeosciences.net/17/1033/2020/, 2020.

Kurbatova, J., Li, C., Varlagin, A., Xiao, X., and Vygodskaya, N.: Modeling Carbon Dynamics in Two Adjacent Spruce Forests with Different Soil Conditions in Russia, Biogeosciences, 5, 969–980, https://doi.org/https://doi.org/10.5194/bg-5-969-2008, 2008.

Lafleur, P. M., Roulet, N. T., Bubier, J. L., Frolking, S., and Moore, T. R.: Interannual variability in the peatland-atmosphere carbon dioxide exchange at an ombrotrophic bog, Global Biogeochemical Cycles, 17, 2003.

Lagergren, F., Lindroth, A., Dellwik, E., Ibrom, A., Lankreijer, H., Launiainen, S., Mölder, M., Kolari, P., Pilegaard, K., and Vesala, T.: Biophysical controls on CO2 fluxes of three Northern forests based on long-term eddy covariance data, Tellus B: Chemical and Physical Meteorology, 60, 143–152, 2008.

Lambert, W. D.: Functional convergence of ecosystems: evidence from body mass distributions of North American late Miocene mammal faunas, Ecosystems, 9, 97–118, 2006.

Lee, J. A., Peluffo-Ordóñez, D. H., and Verleysen, M.: Multi-Scale Similarities in Stochastic Neighbour Embedding: Reducing Dimensionality While Preserving Both Local and Global Structure, Neurocomputing, 169, 246–261, https://doi.org/10.1016/j.neucom.2014.12.095, 2015.

Leon, E., Vargas, R., Bullock, S., Lopez, E., Panosso, A. R., and La Scala, N.: Hot spots, hot moments, and spatio-temporal controls on soil CO2 efflux in a water-limited ecosystem, Soil Biology and Biochemistry, 77, 12 – 21, https://doi.org/https://doi.org/10.1016/j.soilbio.2014.05.029, http://www.sciencedirect.com/science/article/pii/S0038071714002004, 2014.

Leuning, R., Cleugh, H. A., Zegelin, S. J., and Hughes, D.: Carbon and Water Fluxes over a Temperate Eucalyptus Forest and a Tropical Wet/Dry Savanna in Australia: Measurements and Comparison with MODIS Remote Sensing Estimates, Agricultural and Forest Meteorology, 129, 151–173, https://doi.org/https://doi.org/10.1016/j.agrformet.2004.12.004, 2005.

Lindauer, M., Schmid, H. P., Grote, R., Mauder, M., Steinbrecher, R., and Wolpert, B.: Net Ecosystem Exchange over a Non-Cleared Wind-Throw-Disturbed Upland Spruce Forest—Measurements and Simulations, Agricultural and Forest Meteorology, 197, 219–234, https://doi.org/10.1016/j.agrformet.2014.07.005, 2014.

Loubet, B., Laville, P., Lehuger, S., Larmanou, E., Fléchard, C., Mascher, N., Genermont, S., Roche, R., Ferrara, R. M., Stella, P., Personne, E., Durand, B., Decuq, C., Flura, D., Masson, S., Fanucci, O., Rampon, J.-N., Siemens, J., Kindler, R., Gabrielle, B., Schrumpf, M., and Cellier, P.: Carbon, Nitrogen and Greenhouse Gases Budgets over a Four Years Crop Rotation in Northern France, Plant and Soil, 343, 109, https://doi.org/10.1007/s11104-011-0751-9, 2011.

Lund, M., Falk, J. M., Friborg, T., Mbufong, H. N., Sigsgaard, C., Soegaard, H., and Tamstorf, M. P.: Trends in CO2 Exchange in a High Arctic Tundra Heath, 2000–2010, Journal of Geophysical Research: Biogeosciences, 117, https://doi.org/10.1029/2011JG001901, 2012.

Luyssaert, S., Inglima, I., Jung, M., Richardson, A. D., Reichstein, M., Papale, D., Piao, S., Schulze, E.-D., Wingate, L., Matteucci, G., et al.: CO2 balance of boreal, temperate, and tropical forests derived from a global database, Global change biology, 13, 2509–2537, 2007.

Maaten, L. v. d. and Hinton, G.: Visualizing data using t-SNE, Journal of machine learning research, 9, 2579–2605, 2008.

Marcolla, B., Pitacco, A., and Cescatti, A.: Canopy Architecture and Turbulence Structure in a Coniferous Forest, Boundary-Layer Meteorology, 108, 39–59, https://doi.org/10.1023/A:1023027709805, 2003.

Marcolla, B., Cescatti, A., Montagnani, L., Manca, G., Kerschbaumer, G., and Minerbi, S.: Importance of advection in the atmospheric CO2 exchanges of an alpine forest, Agricultural and Forest Meteorology, 130, 193–206, 2005.

Marcolla, B., Cescatti, A., Manca, G., Zorer, R., Cavagna, M., Fiora, A., Gianelle, D., Rodeghiero, M., Sottocornola, M., and Zampedri, R.: Climatic Controls and Ecosystem Responses Drive the Inter-Annual Variability of the Net Ecosystem Exchange of an Alpine Meadow, Agricultural and Forest Meteorology, 151, 1233–1243, https://doi.org/10.1016/j.agrformet.2011.04.015, 2011.

Marengo, J. A., Alves, L. M., Alvala, R., Cunha, A. P., Brito, S., and Moraes, O. L.: Climatic characteristics of the 2010-2016 drought in the semiarid Northeast Brazil region, Anais da Academia Brasileira de Ciências, 90, 1973–1985, 2018.

Matsumoto, K., Ohta, T., Nakai, T., Kuwada, T., Daikoku, K., Iida, S., Yabuki, H., Kononov, A. V., van der Molen, M. K., Kodama, Y., Maximov, T. C., Dolman, A. J., and Hattori, S.: Energy Consumption and Evapotranspiration at Several Boreal and Temperate Forests in the Far East, Agricultural and Forest Meteorology, 148, 1978–1989, https://doi.org/10.1016/j.agrformet.2008.09.008, 2008.

McDowell, N. G., Bowling, D. R., Bond, B. J., Irvine, J., Law, B. E., Anthoni, P., and Ehleringer, J. R.: Response of the Carbon Isotopic Content of Ecosystem, Leaf, and Soil Respiration to Meteorological and Physiological Driving Factors in a Pinus Ponderosa Ecosystem, Global Biogeochemical Cycles, 18, https://doi.org/10.1029/2003GB002049, 2004.

McInnes, L., Healy, J., and Melville, J.: UMAP: Uniform Manifold Approximation and Projection for Dimension Reduction, 2018.

McPherson, R. A.: A review of vegetation—atmosphere interactions and their influences on mesoscale phenomena, Progress in Physical Geography, 31, 261–285, https://doi.org/10.1177/0309133307079055, https://doi.org/10.1177/0309133307079055, 2007.

Medlyn, B. E., Berbigier, P., Clement, R., Grelle, A., Loustau, D., Linder, S., Wingate, L., Jarvis, P. G., Sigurdsson, B. D., and McMurtrie, R. E.: Carbon balance of coniferous forests growing in contrasting climates: Model-based analysis, Agricultural and Forest Meteorology, 131, 97–124, 2005.

Meinzer, F. C.: Functional convergence in plant responses to the environment, Oecologia, 134, 1–11, 2003.

Merbold, L., Ardö, J., Arneth, A., Scholes, R. J., Nouvellon, Y., de Grandcourt, A., Archibald, S., Bonnefond, J. M., Boulain, N., Brueggemann, N., Bruemmer, C., Cappelaere, B., Ceschia, E., El-Khidir, H. a. M., El-Tahir, B. A., Falk, U., Lloyd, J., Kergoat, L., Dantec, V. L., Mougin, E., Muchinda, M., Mukelabai, M. M., Ramier, D., Roupsard, O., Timouk, F., Veenendaal, E. M., and Kutsch, W. L.: Precipitation as Driver of Carbon Fluxes in 11 African Ecosystems, Biogeosciences, 6, 1027–1041, https://doi.org/https://doi.org/10.5194/bg-6-1027-2009, 2009.

Merbold, L., Eugster, W., Stieger, J., Zahniser, M., Nelson, D., and Buchmann, N.: Greenhouse Gas Budget (CO2, CH4 and N2O) of Intensively Managed Grassland Following Restoration, Global Change Biology, 20, 1913–1928, https://doi.org/10.1111/gcb.12518, 2014.

Meyer, W. S., Kondrlova, E., and Koerber, G. R.: Evaporation of Perennial Semi-Arid Woodland in Southeastern Australia Is Adapted for Irregular but Common Dry Periods, Hydrological Processes, 29, {3714–3726}, https://doi.org/{10.1002/hyp.10467}, 2015.

Meyers, T. P. and Hollinger, S. E.: An assessment of storage terms in the surface energy balance of maize and soybean, Agricultural and Forest Meteorology, 125, 105–115, 2004.

Miralles, D. G., Gentine, P., Seneviratne, S. I., and Teuling, A. J.: Land–atmospheric feedbacks during droughts and heatwaves: state of the science and current challenges, Annals of the New York Academy of Sciences, 1436, 19, 2019.

Moors, E. J.: Water Use of Forests in the Netherlands, Tech. Rep. 41, Vrije Universiteit, Amsterdam, 2012.

Moureaux, C., Debacq, A., Bodson, B., Heinesch, B., and Aubinet, M.: Annual Net Ecosystem Carbon Exchange by a Sugar Beet Crop, Agricultural and Forest Meteorology, 139, 25–39, https://doi.org/https://doi.org/10.1016/j.agrformet.2006.05.009, 2006.

Musavi, T., Migliavacca, M., Reichstein, M., Kattge, J., Wirth, C., Black, T. A., Janssens, I., Knohl, A., Loustau, D., Roupsard, O., et al.: Stand age and species richness dampen interannual variation of ecosystem-level photosynthetic capacity, Nature ecology & evolution, 1, 0048, 2017.

Nagy, Z., Czóbel, S., Balogh, J., Horváth, L., Fóti, S., Pintér, K., Weidinger, T., Csintalan, Z., and Tuba, Z.: Some preliminary results of the Hungarian grassland ecological research: carbon cycling and greenhouse gas balances under changing, Cereal Research Communications, 33, 279–281, 2005.

Nardino, M., Georgiadis, T., Rossi, F., Ponti, F., Miglietta, F., and Magliulo, V.: Primary productivity and evapotranspiration of a mixed forest, in: Congress CNR-ISA Fo., Istituto per i Sistemi Agricoli e Forestali del Mediterraneo, Portici, pp. 24–25, 2002.

Nave, L. E., Gough, C. M., Maurer, K. D., Bohrer, G., Hardiman, B. S., Moine, J. L., Munoz, A. B., Nadelhoffer, K. J., Sparks, J. P., Strahm, B. D., Vogel, C. S., and Curtis, P. S.: Disturbance and the Resilience of Coupled Carbon and Nitrogen Cycling in a North Temperate Forest, Journal of Geophysical Research: Biogeosciences, 116, https://doi.org/10.1029/2011JG001758, 2011.

Nelson, J. A., Pérez-Priego, O., Zhou, S., Poyatos, R., Zhang, Y., Blanken, P. D., Gimeno, T. E., Wohlfahrt, G., Desai, A. R., Gioli, B., Limousin, J.-M., Bonal, D., Paul-Limoges, E., Scott, R. L., Varlagin, A., Fuchs, K., Montagnani, L., Wolf, S., Delpierre, N., Berveiller, D., Gharun, M., Belelli Marchesini, L., Gianelle, D., Šigut, L., Mammarella, I., Siebicke, L., Andrew Black, T., Knohl, A., Hörtnagl, L., Magliulo, V., Besnard, S., Weber, U., Carvalhais, N., Migliavacca, M., Reichstein, M., and Jung, M.: Ecosystem transpiration and evaporation: Insights from three water flux partitioning methods across FLUXNET sites, Global Change Biology, 00, https://doi.org/10.1111/gcb.15314, https://onlinelibrary.wiley.com/doi/abs/10.1111/gcb.15314, 2020.

NOAA: National Centers for Environmental Information, State of the Climate: National Climate Report for Annual 2014, published online January 2015, retrieved on August 4, 2020 from https://www.ncdc.noaa.gov/sotc/national/201413.

Papagiannopoulou, C., Miralles, D. G., Decubber, S., Demuzere, M., Verhoest, N. E. C., Dorigo, W. A., and Waegeman, W.: A non-linear Granger-causality framework to investigate climate–vegetation dynamics, Geoscientific Model Development, 10, 1945–1960, https://doi.org/10.5194/gmd-10-1945-2017, https://www.geosci-model-dev.net/10/1945/2017/, 2017a.

Papagiannopoulou, C., Miralles, D. G., Dorigo, W. A., Verhoest, N. E. C., Depoorter, M., and Waegeman, W.: Vegetation anomalies caused by antecedent precipitation in most of the world, Environmental Research Letters, 12, 074 016, http://stacks.iop.org/1748-9326/12/i=7/a=074016, 2017b.

Papale, D., Reichstein, M., Aubinet, M., Canfora, E., Bernhofer, C., Kutsch, W., Longdoz, B., Rambal, S., Valentini, R., Vesala, T., et al.: Towards a standardized processing of Net Ecosystem Exchange measured with eddy covariance technique: algorithms and uncertainty estimation, Biogeosciences, 3, 571–583, 2006.

Pastorello, G., Trotta, C., Canfora, E., Chu, H., Christianson, D., Cheah, Y.-W., Poindexter, C., Chen, J., Elbashandy, A., Humphrey, M., et al.: The FLUXNET2015 dataset and the ONEFlux processing pipeline for eddy covariance data, Scientific data, 7, 1–27, 2020.

Pearson, K.: On Lines and Planes of Closest Fit to Systems of Points in Space, Philosophical Magazine, 2, 559–572, 1901.

Pilegaard, K., Ibrom, A., Courtney, M. S., Hummelshøj, P., and Jensen, N. O.: Increasing Net CO2 Uptake by a Danish Beech Forest during the Period from 1996 to 2009, Agricultural and Forest Meteorology, 151, 934–946, https://doi.org/10.1016/j.agrformet.2011.02.013, 2011.

Potter, B. E., Teclaw, R. M., and Zasada, J. C.: The Impact of Forest Structure on Near-Ground Temperatures during Two Years of Contrasting Temperature Extremes, Agricultural and Forest Meteorology, 106, 331–336, https://doi.org/10.1016/S0168-1923(00)00220-3, 2001.

Potts, D. L., Barron-Gafford, G. A., and Scott, R. L.: Ecosystem hydrologic and metabolic flashiness are shaped by plant community traits and precipitation, Agricultural and Forest Meteorology, 279, 107 674, https://doi.org/https://doi.org/10.1016/j.agrformet.2019.107674, http://www.sciencedirect.com/science/article/pii/S0168192319302904, 2019.

Prescher, A.-K., Grünwald, T., and Bernhofer, C.: Land Use Regulates Carbon Budgets in Eastern Germany: From NEE to NBP, Agricultural and Forest Meteorology, 150, 1016–1025, https://doi.org/10.1016/j.agrformet.2010.03.008, 2010a.

Prescher, A.-K., Grünwald, T., and Bernhofer, C.: Land Use Regulates Carbon Budgets in Eastern Germany: From NEE to NBP, Agricultural and Forest Meteorology, 150, 1016–1025, https://doi.org/10.1016/j.agrformet.2010.03.008, 2010b.

Pryor, S. C., Barthelmie, R. J., and Jensen, B.: Nitrogen Dry Deposition at an AmeriFlux Site in a Hardwood Forest in the Midwest, Geophysical Research Letters, 26, 691–694, https://doi.org/10.1029/1999GL900066, 1999.

Rambal, S., Joffre, R., Ourcival, J. M., Cavender-Bares, J., and Rocheteau, A.: The Growth Respiration Component in Eddy CO2 Flux from a Quercus Ilex Mediterranean Forest, Global Change Biology, 10, 1460–1469, https://doi.org/10.1111/j.1365-2486.2004.00819.x, 2004.

Rayment, M. B. and Jarvis, P. G.: Seasonal Gas Exchange of Black Spruce Using an Automatic Branch Bag System, Canadian Journal of Forest Research, 29, 1528–1538, https://doi.org/10.1139/x99-130, 1999a.

Rayment, M. B. and Jarvis, P. G.: Seasonal Gas Exchange of Black Spruce Using an Automatic Branch Bag System, Canadian Journal of Forest Research, 29, 1528–1538, https://doi.org/10.1139/x99-130, 1999b.

Reich, P. B., Walters, M. B., Ellsworth, D. S., Vose, J. M., Volin, J. C., Gresham, C., and Bowman, W. D.: Relationships of Leaf Dark Respiration to Leaf Nitrogen, Specific Leaf Area and Leaf Life-Span: A Test across Biomes and Functional Groups, Oecologia, 114, 471–482, https://doi.org/10.1007/s004420050471, 1998.

Reichstein, M., Tenhunen, J. D., Roupsard, O., Ourcival, J.-m., Rambal, S., Miglietta, F., Peressotti, A., Pecchiari, M., Tirone, G., and Valentini, R.: Severe drought effects on ecosystem CO2 and H2O fluxes at three Mediterranean evergreen sites: revision of current hypotheses?, Global Change Biology, 8, 999–1017, 2002.

Reichstein, M., Falge, E., Baldocchi, D., Papale, D., Aubinet, M., Berbigier, P., Bernhofer, C., Buchmann, N., Gilmanov, T., Granier, A., Grünwald, T., Havránková, K., Ilvesniemi, H., Janous, D., Knohl, A., Laurila, T., Lohila, A., Loustau, D., Matteucci, G., Meyers, T., Miglietta, F., Ourcival, J.-M., Pumpanen, J., Rambal, S., Rotenberg, E., Sanz, M., Tenhunen, J., Seufert, G., Vaccari, F., Vesala, T., Yakir, D., and Valentini, R.: On the separation of net ecosystem exchange into assimilation and ecosystem respiration: review and improved algorithm, Global Change Biology, 11, 1424–1439, https://doi.org/10.1111/j.1365-2486.2005.001002.x, https://onlinelibrary.wiley.com/doi/abs/10.1111/j.1365-2486.2005.001002.x, 2005.

Reichstein, M., Bahn, M., Mahecha, M. D., Kattge, J., and Baldocchi, D. D.: Linking plant and ecosystem functional biogeography, Proceedings of the National Academy of Sciences, 111, 13 697–13 702, 2014.

Rey, A., Pegoraro, E., Tedeschi, V., Parri, I. D., Jarvis, P. G., and Valentini, R.: Annual Variation in Soil Respiration and Its Components in a Coppice Oak Forest in Central Italy, Global Change Biology, 8, 851–866, https://doi.org/10.1046/j.1365-2486.2002.00521.x, 2002.

Reynolds, J. F., Kemp, P. R., Ogle, K., and Fernández, R. J.: Modifying the 'pulse–reserve'paradigm for deserts of North America: precipitation pulses, soil water, and plant responses, Oecologia, 141, 194–210, 2004.

Rodrigues, A., Pita, G., Mateus, J., Kurz-Besson, C., Casquilho, M., Cerasoli, S., Gomes, A., and Pereira, J.: Eight years of continuous carbon fluxes measurements in a Portuguese eucalypt stand under two main events: Drought and felling, Agricultural and Forest Meteorology, 151, 493–507, 2011.

Rothstein, D. E., Zak, D. R., Pregitzer, K. S., and Curtis, P. S.: Kinetics of Nitrogen Uptake by Populus Tremuloides in Relation to Atmospheric CO2 and Soil Nitrogen Availability, Tree Physiology, 20, 265–270, https://doi.org/10.1093/treephys/20.4.265, 2000.

Ruddell, B. L. and Kumar, P.: Ecohydrologic process networks: 1. Identification, Water Resources Research, 45, n/a–n/a, https://doi.org/10.1029/2008WR007279, http://dx.doi.org/10.1029/2008WR007279, w03419, 2009.

Ruehr, N. K., Martin, J. G., and Law, B. E.: Effects of Water Availability on Carbon and Water Exchange in a Young Ponderosa Pine Forest: Above- and Belowground Responses, Agricultural and Forest Meteorology, 164, 136–148, https://doi.org/10.1016/j.agrformet.2012.05.015, 2012a.

Ruehr, N. K., Martin, J. G., and Law, B. E.: Effects of Water Availability on Carbon and Water Exchange in a Young Ponderosa Pine Forest: Above- and Belowground Responses, Agricultural and Forest Meteorology, 164, 136–148, https://doi.org/10.1016/j.agrformet.2012.05.015, 2012b.

Ruehr, N. K., Martin, J. G., and Law, B. E.: Effects of Water Availability on Carbon and Water Exchange in a Young Ponderosa Pine Forest: Above- and Belowground Responses, Agricultural and Forest Meteorology, 164, 136–148, https://doi.org/10.1016/j.agrformet.2012.05.015, 2012c.

Ruehr, N. K., Martin, J. G., and Law, B. E.: Effects of Water Availability on Carbon and Water Exchange in a Young Ponderosa Pine Forest: Above- and Belowground Responses, Agricultural and Forest Meteorology, 164, 136–148, https://doi.org/10.1016/j.agrformet.2012.05.015, 2012d.

Ruehr, N. K., Martin, J. G., and Law, B. E.: Effects of Water Availability on Carbon and Water Exchange in a Young Ponderosa Pine Forest: Above- and Belowground Responses, Agricultural and Forest Meteorology, 164, 136–148, https://doi.org/10.1016/j.agrformet.2012.05.015, 2012e.

Runge, J.: Causal network reconstruction from time series: From theoretical assumptions to practical estimation, Chaos: An Interdisciplinary Journal of Nonlinear Science, 28, 075 310, https://doi.org/10.1063/1.5025050, https://doi.org/10.1063/1.5025050, 2018.

Runge, J., Bathiany, S., Bollt, E., Camps-Valls, G., Coumou, D., Deyle, E., Glymour, C., Kretschmer, M., Mahecha, M. D., Muñoz-Marí, J., et al.: Inferring causation from time series in Earth system sciences, Nature communications, 10, 2553, 2019a.

Runge, J., Nowack, P., Kretschmer, M., Flaxman, S., and Sejdinovic, D.: Detecting and quantifying causal associations in large nonlinear time series datasets, Science Advances, 5, 2019b.

Sagerfors, J., Lindroth, A., Grelle, A., Klemedtsson, L., Weslien, P., and Nilsson, M.: Annual CO2 exchange between a nutrient-poor, minerotrophic, boreal mire and the atmosphere, Journal of Geophysical Research: Biogeosciences, 113, https://doi.org/10.1029/2006JG000306, https://agupubs.onlinelibrary.wiley.com/doi/abs/10.1029/2006JG000306, 2008.

Saleska, S. R., Miller, S. D., Matross, D. M., Goulden, M. L., Wofsy, S. C., da Rocha, H. R., de Camargo, P. B., Crill, P., Daube, B. C., de Freitas, H. C., Hutyra, L., Keller, M., Kirchhoff, V., Menton, M., Munger, J. W., Pyle, E. H., Rice, A. H., and Silva, H.: Carbon in Amazon Forests: Unexpected Seasonal Fluxes and Disturbance-Induced Losses, Science, 302, 1554–1557, https://doi.org/10.1126/science.1091165, 2003.

Sanz, M., Carrara, A., Gimeno, C., Bucher, A., and Lopez, R.: Effects of a dry and warm summer conditions on CO2 and energy fluxes from three Mediterranean ecosystems, in: Geophys. Res. Abstr, vol. 6, p. 3239, 2004.

Schade, G. W., Goldstein, A. H., and Lamanna, M. S.: Are Monoterpene Emissions Influenced by Humidity?, Geophysical Research Letters, 26, 2187–2190, https://doi.org/10.1029/1999GL900444.

Schreiber, T.: Measuring Information Transfer, Phys. Rev. Lett., 85, 461–464, https://doi.org/10.1103/PhysRevLett.85.461, https://link.aps.org/doi/10.1103/PhysRevLett.85.461, 2000.

Schuldt, B., Buras, A., Arend, M., Vitasse, Y., Beierkuhnlein, C., Damm, A., Gharun, M., Grams, T. E., Hauck, M., Hajek, P., Hartmann, H., Hiltbrunner, E., Hoch, G., Holloway-Phillips, M., Körner, C., Larysch, E., Lübbe, T., Nelson, D. B., Rammig, A., Rigling, A., Rose, L., Ruehr, N. K., Schumann, K., Weiser, F., Werner, C., Wohlgemuth, T., Zang, C. S., and Kahmen, A.: A first assessment of the impact of the extreme 2018 summer drought on Central European forests, Basic and Applied Ecology, 45, 86 – 103, https://doi.org/https://doi.org/10.1016/j.baae.2020.04.003, http://www.sciencedirect.com/science/article/pii/S1439179120300414, 2020.

Schwalm, C. R., Anderegg, W. R., Michalak, A. M., Fisher, J. B., Biondi, F., Koch, G., Litvak, M., Ogle, K., Shaw, J. D., Wolf, A., et al.: Global patterns of drought recovery, Nature, 548, 202–205, 2017.

Scott, R. L., Huxman, T. E., Cable, W. L., and Emmerich, W. E.: Partitioning of Evapotranspiration and Its Relation to Carbon Dioxide Exchange in a Chihuahuan Desert Shrubland, Hydrological Processes, 20, 3227–3243, https://doi.org/10.1002/hyp.6329, 2006.

Scott, R. L., Cable, W. L., and Hultine, K. R.: The Ecohydrologic Significance of Hydraulic Redistribution in a Semiarid Savanna, Water Resources Research, 44, https://doi.org/10.1029/2007WR006149, 2008.

Shadaydeh, M., Denzler, J., Garcia, Y. G., and Mahecha, M.: Time-Frequency Causal Inference Uncovers Anomalous Events in Environmental Systems, in: German Conference on Pattern Recognition (GCPR), 2019.

Shaver, G. R., Street, L. E., Rastetter, E. B., Van Wijk, M. T., and Williams, M.: Functional convergence in regulation of net CO2 flux in heterogeneous tundra landscapes in Alaska and Sweden, Journal of Ecology, 95, 802–817, https://doi.org/10.1111/j.1365-2745.2007.01259.x, https://besjournals.onlinelibrary.wiley.com/doi/abs/10.1111/j.1365-2745.2007.01259.x, 2007.

Sigut, L., Havrankova, K., Jocher, G., Pavelka, M., Janouš, D., Czerny, R., Stanik, K., and Trusina, J.: FLUXNET2015 CZ-BK2 Bily Kriz grassland, https://doi.org/10.18140/FLX/1440144.

Sippel, S., Forkel, M., Rammig, A., Thonicke, K., Flach, M., Heimann, M., Otto, F. E. L., Reichstein, M., and Mahecha, M. D.: Contrasting and interacting changes in simulated spring and summer carbon cycle extremes in European ecosystems, Environmental Research Letters, 12, 075 006, https://doi.org/10.1088/1748-9326/aa7398, https://doi.org/10.1088%2F1748-9326%2Faa7398, 2017.

Sippel, S., Reichstein, M., Ma, X., Mahecha, M. D., Lange, H., Flach, M., and Frank, D.: Drought, heat, and the carbon cycle: a review, Current Climate Change Reports, 4, 266–286, 2018.

Spirtes, P. and Glymour, C.: An Algorithm for Fast Recovery of Sparse Causal Graphs, Social Science Computer Review, 9, 62–72, https://doi.org/10.1177/089443939100900106, https://doi.org/10.1177/089443939100900106, 1991.

Sugihara, G., May, R., Ye, H., Hsieh, C.-h., Deyle, E., Fogarty, M., and Munch, S.: Detecting Causality in Complex Ecosystems, Science, 338, 496–500, https://doi.org/10.1126/science.1227079, http://science.sciencemag.org/content/338/6106/496, 2012.

Suni, T., Rinne, J., Reissell, A., Altimir, N., Keronen, P., Rannik, U., Dal Maso, M., Kulmala, M., and Vesala, T.: Long-Term Measurements of Surface Fluxes above a Scots Pine Forest in Hyytiala, Southern Finland, 1996-2001, BOREAL ENVIRONMENT RESEARCH, 8, {287–301}, 2003.

Székely, G. J., Rizzo, M. L., and Bakirov, N. K.: Measuring and testing dependence by correlation of distances, Ann. Statist., 35, 2769–2794, https://doi.org/10.1214/009053607000000505, https://doi.org/10.1214/009053607000000505, 2007.

Tamrakar, R., Rayment, M. B., Moyano, F., Mund, M., and Knohl, A.: Implications of structural diversity for seasonal and annual carbon dioxide fluxes in two temperate deciduous forests, Agricultural and Forest Meteorology, 263, 465 – 476, https://doi.org/https://doi.org/10.1016/j.agrformet.2018.08.027, http://www.sciencedirect.com/science/article/pii/S0168192318302934, 2018.

Tang, J., Baldocchi, D. D., Qi, Y., and Xu, L.: Assessing Soil CO2 Efflux Using Continuous Measurements of CO2 Profiles in Soils with Small Solid-State Sensors, Agricultural and Forest Meteorology, 118, 207–220, https://doi.org/10.1016/S0168-1923(03)00112-6, 2003.

Tedeschi, V., Rey, A., Manca, G., Valentini, R., Jarvis, P. G., and Borghetti, M.: Soil respiration in a Mediterranean oak forest at different developmental stages after coppicing, Global Change Biology, 12, 110–121, 2006.

Thomas, S. C., Halpern, C. B., Falk, D. A., Liguori, D. A., and Austin, K. A.: Plant diversity in managed forests: understory responses to thinning and fertilization, Ecological applications, 9, 864–879, 1999a.

Thomas, S. C., Halpern, C. B., Falk, D. A., Liguori, D. A., and Austin, K. A.: Plant diversity in managed forests: understory responses to thinning and fertilization, Ecological applications, 9, 864–879, 1999b.

Thomas, S. C., Halpern, C. B., Falk, D. A., Liguori, D. A., and Austin, K. A.: Plant diversity in managed forests: understory responses to thinning and fertilization, Ecological applications, 9, 864–879, 1999c.

Thum, T., Aalto, T., Laurila, T., Aurela, M., Kolari, P., and Hari, P.: Parametrization of Two Photosynthesis Models at the Canopy Scale in a Northern Boreal Scots Pine Forest, Tellus B, 59, 874–890, https://doi.org/10.1111/j.1600-0889.2007.00305.x, 2007.

Valentini, R., Angelis, P. D., Matteucci, G., Monaco, R., Dore, S., and Mucnozza, G. E. S.: Seasonal Net Carbon Dioxide Exchange of a Beech Forest with the Atmosphere, Global Change Biology, 2, 199–207, https://doi.org/10.1111/j.1365-2486.1996.tb00072.x, 1996.

Valentini, R., Matteucci, G., Dolman, A., Schulze, E.-D., Rebmann, C., Moors, E., Granier, A., Gross, P., Jensen, N., Pilegaard, K., et al.: Respiration as the main determinant of carbon balance in European forests, Nature, 404, 861–865, 2000.

van der Molen, M. K., van Huissteden, J., Parmentier, F. J. W., Petrescu, A. M. R., Dolman, A. J., Maximov, T. C., Kononov, A. V., Karsanaev, S. V., and Suzdalov, D. A.: The Growing Season Greenhouse Gas Balance of a Continental Tundra Site in the Indigirka Lowlands, NE Siberia, Biogeosciences, 4, 985–1003, https://doi.org/https://doi.org/10.5194/bg-4-985-2007, 2007.

Vitale, L., Di Tommasi, P., D'Urso, G., and Magliulo, V.: The Response of Ecosystem Carbon Fluxes to LAI and Environmental Drivers in a Maize Crop Grown in Two Contrasting Seasons, International Journal of Biometeorology, 60, 411–420, https://doi.org/10.1007/s00484-015-1038-2, 2016.

von Buttlar, J., Zscheischler, J., Rammig, A., Sippel, S., Reichstein, M., Knohl, A., Jung, M., Menzer, O., Arain, M. A., Buchmann, N., Cescatti, A., Gianelle, D., Kiely, G., Law, B. E., Magliulo, V., Margolis, H., McCaughey, H., Merbold, L., Migliavacca, M., Montagnani, L., Oechel, W., Pavelka, M., Peichl, M., Rambal, S., Raschi, A., Scott, R. L., Vaccari, F. P., van Gorsel, E., Varlagin, A., Wohlfahrt, G., and Mahecha, M. D.: Impacts of droughts and extreme-temperature events on gross primary production and ecosystem respiration: a systematic assessment across ecosystems and climate zones, Biogeosciences, 15, 1293–1318, https://doi.org/10.5194/bg-15-1293-2018, https://www.biogeosciences.net/15/1293/2018/, 2018.

Wagg, C., O'Brien, M. J., Vogel, A., Scherer-Lorenzen, M., Eisenhauer, N., Schmid, B., and Weigelt, A.: Plant diversity maintains long-term ecosystem productivity under frequent drought by increasing short-term variation, Ecology, 98, 2952–2961, https://doi.org/10.1002/ecy.2003, https://esajournals.onlinelibrary.wiley.com/doi/abs/10.1002/ecy.2003, 2017.

Wales, S. B., Kreider, M. R., Atkins, J., Hulshof, C. M., Fahey, R. T., Nave, L. E., Nadelhoffer, K. J., and Gough, C. M.: Stand age, disturbance history and the temporal stability of forest production, Forest Ecology and Management, 460, 117 865, https://doi.org/https://doi.org/10.1016/j.foreco.2020.117865, http://www.sciencedirect.com/science/article/pii/S0378112719315191, 2020.

Wang, C., Bond-Lamberty, B., and Gower, S. T.: Environmental Controls on Carbon Dioxide Flux from Black Spruce Coarse Woody Debris, Oecologia, 132, 374–381, https://doi.org/10.1007/s00442-002-0987-4, 2002a.

Wang, C., Bond-Lamberty, B., and Gower, S. T.: Environmental Controls on Carbon Dioxide Flux from Black Spruce Coarse Woody Debris, Oecologia, 132, 374–381, https://doi.org/10.1007/s00442-002-0987-4, 2002b.

Wang, C., Bond-Lamberty, B., and Gower, S. T.: Environmental Controls on Carbon Dioxide Flux from Black Spruce Coarse Woody Debris, Oecologia, 132, 374–381, https://doi.org/10.1007/s00442-002-0987-4, 2002c.

Westergaard-Nielsen, A., Lund, M., Hansen, B. U., and Tamstorf, M. P.: Camera Derived Vegetation Greenness Index as Proxy for Gross Primary Production in a Low Arctic Wetland Area, ISPRS Journal of Photogrammetry and Remote Sensing, 86, 89–99, https://doi.org/10.1016/j.isprsjprs.2013.09.006, 2013.

Wofsy, S. C., Goulden, M. L., Munger, J. W., Fan, S.-M., Bakwin, P. S., Daube, B. C., Bassow, S. L., and Bazzaz, F. A.: Net Exchange of CO2 in a Mid-Latitude Forest, Science, 260, 1314–1317, https://doi.org/10.1126/science.260.5112.1314, 1993.

Wohlfahrt, G., Hammerle, A., Haslwanter, A., Bahn, M., Tappeiner, U., and Cernusca, A.: Seasonal and inter-annual variability of the net ecosystem CO2 exchange of a temperate mountain grassland: Effects of weather and management, Journal of Geophysical Research: Atmospheres, 113, 2008.

Xu, L., Baldocchi, D. D., and Tang, J.: How Soil Moisture, Rain Pulses, and Growth Alter the Response of Ecosystem Respiration to Temperature, Global Biogeochemical Cycles, 18, https://doi.org/10.1029/2004GB002281, 2004.

Yi, C., Davis, K. J., Berger, B. W., and Bakwin, P. S.: Long-Term Observations of the Dynamics of the Continental Planetary Boundary Layer, Journal of the Atmospheric Sciences, 58, 1288–1299, https://doi.org/10.1175/1520-0469(2001)058<1288:LTOOTD>2.0.CO;2, 2001.

Zeller, K. and Hehn, T.: Measurements of Upward Turbulent Ozone Fluxes above a Subalpine Spruce-Fir Forest, Geophysical Research Letters, 23, 841–844, 1996.

Zeller, K. F. and Nikolov, N. T.: Quantifying Simultaneous Fluxes of Ozone, Carbon Dioxide and Water Vapor above a Subalpine Forest Ecosystem, Environmental Pollution, 107, 1–20, https://doi.org/10.1016/S0269-7491(99)00156-6, 2000.

Zielis, S., Etzold, S., Zweifel, R., Eugster, W., Haeni, M., and Buchmann, N.: NEP of a Swiss Subalpine Forest Is Significantly Driven Not Only by Current but Also by Previous Year's Weather, Biogeosciences, 11, 1627–1635, https://doi.org/https://doi.org/10.5194/bg-11-1627-2014, 2014.

Zscheischler, J., Martius, O., Westra, S., Bevacqua, E., Raymond, C., Horton, R. M., van den Hurk, B., AghaKouchak, A., Jézéquel, A., Mahecha, M. D., et al.: A typology of compound weather and climate events, Nature reviews earth & environment, pp. 1–15, 2020.